A LINEAR SOLUTION FOR THE JET FLAP IN GROUND EFFECT

Thesis by

Peter B. S. Lissaman

In Partial Fulfillment of the Requirements

For the Degree of

Doctor of Philosophy

California Institute of Technology

Pasadena, California

1966

Submitted 7 December 1965

ACKNOWLEDGMENTS

The writer would like to express his gratitude to Dr. Homer J. Stewart for his continuous advice and encouragement. He would also like to thank Dr. Theodore T-Y. Wu for suggesting the problem, and Dr. Frank E. Marble for his perceptive and constructive help.

ABSTRACT

The paper presents the solution of the problem of the Jet Flap airfoil in a plane inviscid flow in the presence of the ground.

The basic flow equations are derived and the non-linearity of the boundary conditions are discussed. The problem is then linearized as in thin airfoil theory. By a conformal transformation the flow field is mapped into one having very simple geometry. The singularities of the mapping are identified and the asymptotic character of the flow fields derived. The basic integro-differential equation is developed; this has singular Hilbert type kernels and discontinuous boundary conditions.

By considerations of the second order effects, significant relationships between the lift slopes with angle of attack, with jet angle and jet coefficient are developed. These are further simplified by introduction of a new geometrical parameter developed from the mapping.

The lift coefficient of the airfoil is expressed in three parts, of which two may be evaluated in simple closed form. The remaining part depends on the solution of the integro-differential equation. This equation is then solved at N points by assuming a piecewise smooth velocity distribution and generating an N x N matrix: numerical results are obtained from an IBM 7094 computer. It is proved that this approximation converges to the exact solution.

The limiting cases, when the height to chord ratio, h/c, or jet coefficient, C_J, approach zero or infinity are developed, exploiting the decomposition of the lifting components; and an asymptotic

result for small C_J is presented.

A linearized theory for wake blockage is given, which also gives an indication of the restrictions on the various parameters implied by the basic linear approach.

The results for $h/c \rightarrow \infty$ correlate excellently with Spence's solution for $h/c = \infty$. For low values of h/c the results agree quite well with the limited applicable test data.

TABLE OF CONTENTS

TABLE OF CONTENTS (Cont'd.)

TABLE OF CONTENTS (Cont'd.)

I. INTRODUCTION

A. BASIC PRINCIPLES AND BACKGROUND

Although the concept of the Jet Flap is an old one, and was mentioned in principle by Prandtl, it is only within the last decade that it has been seriously studied: mainly because the gas turbine has made readily available the high energy jet air required. The earliest writers, for example Davidson (Ref. 1), commented on the remarkable characteristics of the device. In essence, these consist of an order of magnitude theoretical increase in maximum lift coefficient (and lift slope) with zero additional power requirements in the two-dimensional case. Experimental tests have shown that both these effects are actually realized to a very high degree.

The lift increase occurs in principle from the fact that the jet wake effectively extends the airfoil lifting surface. Alternately, this may be regarded as an extra lifting component due to the downward deflected jet, but it should be noted that in addition to this direct momentum lift, there is an appreciable increment of pressure lift, induced on the airfoil itself. Now the conventional airfoil is prevented from achieving its maximum theoretical lift, which is about 2π, by boundary layer separation due to strong adverse pressure gradients on the upper surface. In the case of the Jet Flap, however, a favorable gradient is induced on the rear portion of the airfoil (Fig. 1), which makes the airfoil behave very similarly to the theoretical inviscid predictions. There is still an area of possible separation near the airfoil leading edge but this is in a

region where the boundary layer is in a 'healthy' state, and separation may usually be controlled either by geometrical means or by surface transpiration. As an illustration of the correlation of theory and experiment, because of negligible viscous interaction, we note in Ref. 2 that at a C_L of 6 the measured experimental value is within 5% of the inviscid prediction.

The fact that this lift requires no extra power, or more precisely that the jet momentum required to produce the jet lift effect is completely recovered in thrust, has been the source of much debate and is in fact known as the thrust hypothesis. This was first proposed by Davidson and Stratford (Ref. 3), using arguments based on momentum concepts and has been fully justified by more advanced potential-theoretic methods by Spence (Ref. 2). Recent experiments by Foley (Ref. 4) have shown that, within limits imposed by dissipation due to real effects, the thrust hypothesis is realized even for large angles of jet deflection.

It will be evident that the Jet Flap shows great potential for all aerial vehicles requiring high lift coefficients in some portion of their flight envelope. In particular, the fact that in theory there is only a small thrust loss in the Jet Flap mass flow makes it possible to visualize the use of extensive lift augmentation for takeoff as well as landing. It may also be noted that Jet Flap principles provide very powerful lift amplification for control surfaces; producing higher control effectiveness than either plain reaction control nozzles or simple flaps. This is particularly pertinent in the very high and low speed flight regimes.

Thus the Jet Flap is directly applicable not only to V/STOL devices, but also to subsonic and supersonic vehicles of the conventional type. It has also been proposed as a solution to the mechanical problems associated with cyclic and collective pitch control on helicopter rotors; where the property that the lift may be varied independently of angle of attack may be exploited, by changing either the jet momentum coefficient, C_J, or the jet angle, θ. The application of Jet Flap principles has made GEM and Hovercraft vehicles possible.

Technologically, a theoretical prediction of Jet Flap performance is of importance. For the case of an infinite fluid this is well provided (at least in the linear inviscid case) by the papers referred to in the next section. The influence of the ground plane, however, has a large effect and this is still appreciable even when the airfoil is fairly high above the ground. For example, from the results of this paper we show that if we define a ground induced increment in lift slope by ΔC_{L_α} $(= C_{L_\alpha}{}_{h/c = 1.18} - C_{L_\alpha}{}_{h/c = \infty})$ we obtain without blowing:

$$\Delta C_{L_\alpha} \approx .20 \qquad (C_J = 0)$$

while with blowing

$$\Delta C_{L_\alpha} \approx .75 \qquad (C_J = 1.0)$$

B. THEORETICAL DEVELOPMENTS

The Jet Flap behaves unlike an ordinary airfoil in many respects. In particular, the Kutta Condition -- in the sense of zero loading at the trailing edge -- no longer applies; nor does the other familiar airfoil characteristic, that of a constant lift slope. In addition to the normal airfoil parameters of angle of attack, thickness and camber we must add the jet coefficient and the jet angle.

An analytical formulation of the problem leads one to an integro-differential equation with singular kernels and discontinuous boundary conditions. The kernel, of the Hilbert type, causes no serious difficulty: but the boundary discontinuity introduces logarithmic singularities which, although weak, cannot be eliminated analytically. The physical reason for the integro-differential quality of the governing equation is that the shape of the jet wake is unknown in advance and both determines and is determined by the local pressure distribution.

Some theoretical approaches have been made assuming a jet shape, which converts the problem to one of a potential field with Neumann boundary conditions. By retaining only one arbitrary constant, determined from experiment, Pivko (Ref. 5) has obtained good correlation with experiment, however this has theoretical inadequacies in that this constant is intimately related to the jet wake decay, which is the very heart of the basic problem.

An elegant solution of the full integro-differential equation,

under the usual linearizations of thin airfoil theory has been given by Spence (Ref. 2), while the unsteady case has been treated by Erickson (Ref. 6). Both these theories are for the two-dimensional jet flap in an inviscid fluid. A general theory for the three-dimensional jet-flapped wing is given by Das (Ref. 7) in which he uses, as a foundation, the basic Spence two-dimensional solutions.

Special cases of the influence of ground effect are given by Huggett (Ref. 8) and Williams (Ref. 9). These papers do not consider the integro-differential character of the basic flow equations, being directed principally at predicting the phenomenon of wake blockage.

A preliminary approach to the exact solution of the problem with ground effect is made by the writer in Ref. 10. The present paper amplifies and extends this technique to provide an exact solution to the problem. The procedure is outlined below.

Having linearized the problem in the real z plane and formulated the kinematic and dynamic boundary conditions there, we map conformally into an auxiliary ζ plane, thus greatly simplifying the geometry. In the ζ plane we have the problem of determining an analytic function defined in the upper half plane by boundary conditions on the line $\mathcal{I}(\zeta) = 0$. The boundary conditions are not given explicitly, but in the Riemann-Hilbert-Poincare form, i.e., as

$$\mathcal{R}\left(w(\zeta) + if(\zeta)\frac{dw}{d\zeta}\right) = 0 \quad \text{on } C(\zeta)$$

where $w(\zeta)$ is the complex conjugate velocity, f a known function

and $\mathcal{R}$, $\mathcal{I}$ represent the real and imaginary parts of an analytic function. Muskhelishvili (Ref. 11) shows how to convert this to an integro-differential equation; although in this case this does not simplify the problem. A further difficulty in pursuing approaches of Ref. 11 is that our boundary conditions do not satisfy the Hölder condition.

By establishing some elementary superposition theorems it is possible greatly to simplify the character of the integro-differential equation. Of course this cannot eliminate the characteristic difficulties described in the previous paragraph, however, a basic case is developed and the solution of this case provides much information on the more general situation.

From consideration of the global results and the second order effects of the nose singularity some important relationships are established. These enable us both to check the convergence of the numerical solution and to extend the basic case solved to a more general one. Further insight to the asymptotic behaviour of the numerical solution in the ζ plane is obtained by considering the flow at infinity in the real plane.

To solve the basic case we set up an arbitrary linear interpolation for the unknown boundary v distribution and, with the help of the singularities and the asymptotic behaviour, develop a linear matrix equation which may be solved for the unknown distribution. The solution is exact in the sense that any degree of accuracy may be obtained by reducing the step size of the interpolation function, a proof of convergence being given.

By decomposition of the lift coefficient into three parts, it is possible to obtain in addition to the solution in the general range of parameters, asymptotic results for various limiting cases of the height to chord ratio, h/c, and the jet coefficient C_J. Next we obtain some insight into conditions which must be satisfied for the linear theory to be valid, as well as theoretical estimates of the onset of wake blockage.

The analysis of the generalization of the problem for camber and thickness is presented but in this case no numerical solutions are made.

II. ANALYSIS

A. BASIC CONSIDERATIONS AND EQUATIONS

We consider a two-dimensional airfoil in a steady, inviscid, incompressible flow of uniform velocity at infinity, in the presence of an infinite ground plane. A jet of fluid issues from the trailing edge of the airfoil. The basic geometry is sketched in Fig. 1.

Defining a velocity potential Φ for the flow, the considerations mentioned above give us a field equation of the simple Laplace form:

$$\nabla^2 \Phi = 0$$

We notice, however, that not only must boundary conditions be met at the various solid surfaces and at infinity, as is the situation in the classic case, but also that certain special flow conditions must be met on the free boundaries of the jet.

We make the assumption that the jet, of density ρ_J issues from the trailing edge at a high velocity V_J, and of vanishing thickness δ_J such that the mass flow M and the jet momentum J are finite, i.e.,

$$M = \rho_J \delta_J V_J$$

$$J = \rho_J \delta_J V_J^2$$

It can then be shown that within the assumptions (principally that of zero viscosity) the jet may be considered as a curved line, across which there is a discontinuity in both Φ and in the velocity

V_S of the external flow parallel and adjacent to the jet. At the same time there can be no flow through the jet so the external flow has zero velocity normal to the jet. The validity of this assumption is shown by Spence (Ref. 2) and the mathematical justification is further discussed at some length by Erickson (Ref. 6).

As a consequence of the simple kinematic conditions we have the usual boundary condition that the flow must be locally parallel to the airfoil, the jet and the ground plane. If the shape of the jet were known, this would be sufficient to define the problem as being one of the classic Neumann type, i.e., finding a potential flow field given the physical boundaries. However, because of the unknown jet shape, we require an additional condition on the jet. This is provided by the dynamic boundary condition across the jet. To obtain this we consider a small element of the jet and show that for it to be in force equilibrium there must be a pressure differential across it which can be related to the centrifugal force on the jet. Considering the element shown in Fig. 1 we see that

$$\frac{\rho_J \delta_J V_J^2}{R} = P_L - P_U$$

where R is the radius of curvature of the jet and P_L, P_U are the static pressures of the outer flow on the lower and upper surfaces respectively. We now define a jet coefficient

$$C_J = \frac{\rho_J \delta_J V_J^2}{\frac{1}{2}\rho U^2 c}$$

where $\frac{1}{2}\rho U^2$ is the dynamic pressure of the free stream flow and c

the airfoil chord. We then obtain the condition (where C_p is defined in the conventional fashion as $\frac{p-p_o}{\frac{1}{2}\rho U^2}$)

$$\frac{c}{R} C_J = C_{p_L} - C_{p_U}$$

Now, because the external flow is irrotational and of uniform head at infinity we can apply Bernoulli's equation in its most simple form to give

$$C_p = 1 - \frac{V^2}{U^2} = 1 - \frac{(\nabla\Phi)^2}{U^2}$$

where V is the velocity at any point, which can also be expressed as the gradient of Φ, denoted $\nabla\Phi$.

Thus the problem can be formulated as follows: We require a potential Φ, having a field equation $\nabla^2\Phi = 0$ throughout the flow, with the kinematic boundary conditions

$\nabla\Phi \rightarrow U$

$x, y \rightarrow \infty$

$\frac{\partial\Phi}{\partial n} = 0$ on S(x,y), the body surface

on J(x,y), the jet sheet

on G(x,y), the ground plane

and the dynamic boundary conditions

$$(\nabla\Phi_U)^2 - (\nabla\Phi_L)^2 = \frac{cC_J U^2}{R(x,y)}$$ on J(x,y) the jet sheet where R(x,y) is its local radius of curvature.

Now, although Laplace's equation is linear, the problem becomes non-linear because of its boundary conditions, essentially the dynamic condition. A further problem occurs in that the jet boundary conditions must be applied on a curve which is not known in advance, but must be determined by the flow field itself. In this respect the problem has certain similarities to that of gravity waves on a free fluid surface with the jet coefficient playing a role analogous to that of the Froude Number.

We linearize the equations in the customary thin airfoil manner. While this involves assumptions that all flow angles are small, it is known from experience that this gives highly satisfactory results for representative airfoil shapes, except very near the nose. We thus assume both that the velocity perturbations are small, and that the boundary conditions may be applied on some mean plane, instead of the actual surface itself. This means that we now have a linear equation and linear boundary conditions but the boundary condition on the jet sheet is still not explicitly defined but given as a function of the derivative of the dependent variable.

The linearized problem is sketched in Fig. 2.

We now introduce a perturbation potential ϕ and normalize the problem with respect to the free stream velocity. Thus we obtain for the potential Φ

$$\Phi = Ux + \phi$$

with u, v the normalized perturbation velocities defined as

$$u = \frac{1}{U}\phi_x$$

$$v = \frac{1}{U}\phi_y \ .$$

Now on the airfoil and jet boundary we have the kinematic condition

$$\left.\frac{dy}{dx}\right|_{y=h} = \frac{v}{1+u}$$

or, linearizing $\left.\frac{dy}{dx}\right|_{y=h} = y' = v$;

while at infinity $u, v \to 0$.

Then the linearized pressure coefficient becomes -2u, and the linearized radius of curvature $1/y''$ so that the dynamic jet boundary condition may be written

$$u^+ - u^- = \frac{cC_J}{2} y'' \text{ on the jet sheet;}$$

where u^+ represents the perturbation velocity on the upper surface of the sheet and u^- that on the lower. For ϕ itself we again have the Laplacian $\nabla^2\phi = 0$.

Expressing these results more formally we have,

$\phi = \phi(x,y)$,	$\nabla^2\phi = 0$	all x, y
$v = y'^+_a$	$y = h + 0$,	$0 < x < c$
$v = y'^-_a$	$y = h - 0$,	$0 < x < c$
$v = y'_J$	$y = h$,	$c < x$
$v = 0$	$y = 0$,	all x
$u^+ - u^- = \frac{cC_J}{2} y''$	$y = h$,	$c < x$

where $y_a'^+$ is the slope of the airfoil upper surface, $y_a'^-$ that of the lower, and y_J' the slope of the upper or lower surface of the jet.

This represents a potential problem which not only has mixed boundary values but where these values are in part specified in terms of the solution itself. We know v explicitly on the airfoil itself, in terms of its prescribed geometry, but we do not have the corresponding information for the jet sheet.

B. TRANSFORMATION PLANE

Because of the difficulty of the discontinuous boundary conditions on the airfoil and the jet we wish to conformally transform the problem to 'open out' this slit in the plane, at the same time we wish to incorporate the ground plane as part of one continuous simple boundary. For this we use the Schwartz-Christoffel transformation to convert our flow field into that above the half-plane. Defining the transformation plane as the ζ plane where $\zeta = \xi + i\eta$ we see that the transformation derivative must be

$$\frac{dz}{d\zeta} = D \frac{\zeta - a}{\zeta + k}$$

where D is a constant and a, -k are singular points in the ζ plane corresponding to nonconformalities of the mapping, namely the leading edge $z = ih$, and the lower jet at $z = \infty + ih$.

The derivative can be immediately integrated to give

$$z = A_1 \{\zeta - (a+k) \log (\zeta+k)\} + B_1$$

Now we can determine the arbitrary constants A_1, B_1 by specifying that B, C the upper and lower trailing edge (shown in Fig. 2) should transform to +1 and -1 in the ζ plane. Thus we may tabulate the corresponding points below:

z Plane	Point	ζ Plane
ih	A	a
c + i(h+0)	B	+1
c + i(h-0)	C	-1

These conditions provide us with the fully specified transformation

$$z - ih = \frac{h}{(a+k)\pi} \{\zeta - a - (a+k) \log \frac{\zeta+k}{a+k}\} \qquad (1)$$

Because A, B and C have been specified, the point K is not arbitrary and is given implicitly by

$$(a+k) \log \frac{k+1}{k-1} = 2$$

where the point K is located at $\zeta = -k$ in the ζ plane. In addition, the chord of the airfoil in the real plane is expressed by

$$c = \frac{h}{(a+k)\pi} \{1 - a - (a+k) \log \frac{1+k}{a+k}\} \quad .$$

We observe further that the transformation is multivalued along the line $z = ih + x$, $o < x$. This implies that points on this line in the z plane transform to a point pair in the ζ plane. We define then, the two values of ζ corresponding to a given point on this line as ζ^+, ζ^-. These values are both real, and we associate ζ^+ with the point corresponding to $z = x + ih$ on the upper surface of the jet, and ζ^- the lower surface. Thus this transformation removes the flow discontinuity in the z plane and we may now speak of the upper and lower jet sheet surfaces in much the same way as the upper and lower airfoil surfaces.

The basic geometry of the transformation is shown in Fig. 3. A consequence of this transformation is the non linear length scaling between the upper and lower surfaces. We find that the transformed length AK becomes very small in the ζ plane as h/c reduces. This

implies that the upper and lower surface conditions become less and less symmetric as the airfoil approaches the ground plane.

As an indication of this effect the lengths $\ell = k - 1$ and $b = 1 + a$ are plotted on Fig. 4, with the appropriate h/c shown parametrically. It will be seen that values of ℓ less than 10^{-3} are required for h/c less than unity. This introduces numerical complications which are discussed in a later section.

C. BOUNDARY CONDITIONS IN THE ζ PLANE

In the real z plane, we define $w = u - iv$ as the conjugate complex velocity. As is well-known, any analytic function of z, $w = w(z)$ will define a conjugate complex velocity satisfying the conditions of irrotationality and zero divergence. Now if we map the z plane analytically to the ζ plane we observe that the conjugate complex velocity is also an analytic function of ζ. Consequently we define identical boundary conditions on w for corresponding points in the z and ζ planes, then after solving in the ζ plane may transform to the real plane with the assurance that the perturbation potential ϕ in this plane is in fact Laplacian.

Thus the problem becomes that of determining the analytic function $w = u - iv = w(\zeta)$ where w is defined for $\mathcal{I}(\zeta) > 0$ with the boundary conditions on $\mathcal{I}(\zeta) = 0$

$$
\begin{aligned}
v &= 0 && \zeta < -k \\
v &= y_J'^{-} && -k < \zeta < -1 \\
v &= y_a'^{+} && -1 < \xi < a \\
v &= y_a'^{+} && a < \xi < 1 \\
v &= y_J'^{-} && 1 < \xi
\end{aligned}
$$

We now introduce the dynamic condition to develop an equation for v on the jet. This condition is

$$u^+ - u^- = \frac{cC_J}{z} y_J''$$

Since $y_J'' = \frac{dy_J'}{dx} = \frac{dy_J'}{dx} = \frac{dy_J'}{d\zeta} \cdot \frac{d\zeta}{dx}$, and $u^+ = u(\xi^+)$

we get

$$u(\xi^+) - u(\xi^-) = \frac{cC_J}{z} \frac{d\xi^+}{dx} \cdot \frac{dy'_J}{d\xi}, \quad 1 < \xi^+$$

We may now use Poisson's equation for solution of this type of boundary condition giving

$$w(\zeta) = \frac{1}{\pi} \int_{-\infty}^{\infty} \frac{v(t)}{t-\zeta} \, dt$$

Then for $\mathcal{I}(\zeta) = 0+$, $\zeta = \xi$ we get

$$u(\xi) = \frac{-1}{\pi} \oint_{-\infty}^{\infty} \frac{v(t)}{t-\xi} \, dt$$

where $\oint$ represents the Cauchy Principal Value. Hereafter we take all integrals to be the Principal Value if their kernels are singular and drop the special notation on the integral sign.

Thus we obtain an expression for the solution as

$$u(\xi) = \frac{-1}{\pi} \int_{-\infty}^{\infty} \frac{v(t)}{t-\xi} \, dt \qquad \text{all } \xi$$

$$u^+ - u^- = \frac{cC_J}{2} \frac{dv}{d\xi} \frac{d\xi}{dx}, \qquad 1 < \xi$$

with v defined as previously.

The physical boundary conditions are now developed. If the airfoil surface relative to its chord line is given by $y_a = y_c \pm y_t$ with y_c, y_t the camber and thickness coordinates, while α is the angle of attack measured positive in the conventional sense, and τ the jet angle measured relative to the ground plane and positive upwards, then we obtain

$$
\begin{aligned}
v &= 0 && \xi < -k \\
v &= \tau && -k < \xi < -1 \\
v &= -a + y_c' - y_t' && -1 < \xi < a \\
v &= -a + y_c' + y_t' && a < \xi < 1 \\
v &= \tau && 1 < \xi
\end{aligned}
$$

Inserting these conditions into the Poisson Equation, eliminating u by means of the dynamic condition and rearranging we obtain

$$
\begin{aligned}
&\frac{\pi^2}{2}\frac{c}{h}C_J\frac{\xi^+ + k}{\xi^+ - \xi^-}\frac{d\tau}{d\xi} + \int_{-k}^{-1}\frac{\tau(t)}{(t-\xi^+)(t-\xi^-)}\,dt \\
&+\int_{1}^{\infty}\frac{\tau(t)}{(t-\xi^+)(t-\xi^-)}\,dt + \int_{-\infty}^{\infty}\frac{S^*(t,a)}{(t-\xi^+)(t-\xi^-)}\,dt = \\
&\int_{-1}^{+1}\frac{a - y_c'(t)}{(t-\xi^+)(t-\xi^-)}\,dt + \int_{-1}^{a}\frac{y_t'(t)}{(t-\xi^+)(t-\xi^-)}\,dt \\
&\int_{a}^{1}\frac{-y_t'(t)}{(t-\xi^+)(t-\xi^-)}\,dt \quad , \qquad \tau(1) = \tau_1 \qquad \tau(\infty) = 0
\end{aligned}
\tag{2}
$$

Here S*(t,a) is an additional function which may be required because of the mapping singularity at $\xi = a$. S* is a function satisfying the conditions

$$S^*(t,a) = 0 \qquad t \neq a$$

$S^*(a,a)$ unbounded.

It will account for the singularity at the leading edge of the airfoil.

Equation (2) is the basic integro-differential equation of the jet flap in ground effect. It is to be solved for $\xi^+ > 1$ regarding ξ^+ as the independent variable and τ as the unknown with the additional condition $\tau(\xi^+) = \tau(\xi^-)$. Considered as a boundary value problem in analytic functions it is known as the Riemann-Hilbert-Poincare Problem (Mushkelishvili Ref. 11).

D. SUPERPOSITION OF SOLUTIONS

Considering Eq. 2, we observe that the right-hand side, which is prescribed, may be regarded as the input function, together with the jet slope at the trailing edge. Because of the linearity we may break the problem down into a set of superposable solutions as is done in thin airfoil theory. We classify the cases as follows

1. Basic Jet Angle Case

Here we have $y_t = 0$

$y_c = 0$

$\alpha = 0$

$\tau_1 = \tau_b$

and determine a solution τ_τ

2. Angle of Attack Case

Here we have $y_t = 0$

$y_c = 0$

α

$\tau_1 = -\alpha$

and determine a solution τ_α

3. Camber Case

Here we have $y_t = 0$

y_c

$\alpha = 0$

$\tau_1 = y_{c(\xi-1)}$

4. Thickness Case

Here we have y_t

$y_c = 0$

$a = 0$

$\tau_1 = 0$

and determine a solution τ_τ.

If we define the left-hand side of Eq. 2 as $J(\tau)$ where J is a functional of the function τ we get the following equations for the basic cases

$$J(\tau_\tau) = 0 , \qquad \tau_\tau(1) = \tau_b$$

$$J(\tau_a) = a \int_{-1}^{+1} \frac{dt}{(t-\xi^+)(t-\xi^-)} , \quad \tau_a(1) = -a$$

$$J(\tau_c) = \int_{-1}^{+1} \frac{-y'_c(t)}{(t-\xi^+)(t-\xi^-)}\, dt, \quad \tau_c(1) = y'_{c(\xi=1)}$$

$$J(\tau_t) = \int_{-1}^{a} \frac{y'_t(t)}{(t-\xi^+)(t-\xi^-)}\, dt - \int_{a}^{1} \frac{y'_t(t)}{(t-\xi^+)(t-\xi^-)}\, dt, \quad \tau_t(1) = 0$$

E. SINGULARITIES OF THE SOLUTION

In general we expect singularities to occur either where the transformation is singular or where the boundary conditions are discontinuous. The former occurs at $\xi = a$, or at the leading edge of the airfoil and the latter at $\xi \leq 1$ typically due to discontinuous changes in v due to a flap on the airfoil or at the trailing edge due to the jet flap angle itself. In addition, we must consider the nature of the flow at infinity in both planes.

1. Leading Edge Singularity

Considering the flow in the z plane, we note that because there is no net velocity flux in this plane (excluding the jet flux) a circuit taken in the cut plane must give us the result

$$\{zw(z)\} = 0$$

$$z \to \infty$$

Now considering the transformation, we note that, for example, far forward on the ground plane the mapping again becomes linear so that in this region

$$z = \frac{h}{(a+k)\pi}\ \zeta + O(\log(k-\zeta))$$

thus we see $w(\xi) = O(\frac{1}{\xi^2})$ implying that there must be no net source effect in the ζ plane. $\xi \to -\infty$

We now consider the additional u term due to $S^*(\xi, a)$ and see that it must be in the form of a simple pole

$$u(\xi) = -\frac{1}{\pi}\ \frac{N_o}{\xi - a}$$

and because of the above condition of no source terms, we can immediately evaluate N_o which is given by

$$N_o = \int_{-\infty}^{\infty} v(t)dt$$

We refer to N_o as the nose source and obtain further insight on its significance by considering the local flow in the real plane.

We assume the total flow near a is given by

$$u(\xi) = -\frac{N_o}{\pi(\xi-a)} + O(\xi-a)$$

Now the transformation derivative is given by

$$\frac{dx}{d\xi} = \frac{h}{(a+k)\pi} \cdot \frac{\xi-a}{\xi+k}$$

so that near the nose we have

$$x = \frac{h}{(a+k)^2\pi} \frac{(\xi-a)^2}{2} + O(\xi-a)^3$$

Substituting this value into the velocity term we obtain

$$u(x) = \pm \frac{N_o}{2^{1/2}\pi^{3/2}} \cdot \frac{h^{\frac{1}{2}}}{(a+k)} \frac{1}{x^{\frac{1}{2}}}$$

This is the familiar square root singularity of thin airfoil theory.

We see now that the term $S^*(\xi,a)$ may be written $S^*(\xi,a) \equiv N_o \delta(\xi-a)$ or as the Dirac delta function of argument a.

2. Trailing Edge Singularity

At the trailing edge ($\xi = \pm 1$ in the ζ plane) the transformation itself is regular but there are in general discontinuities in the

boundary conditions v and hence in u. For the Basic Jet Angle Case this discontinuity is of magnitude τ_b.

It is easy to show that near $\xi = 1$ we have

$$u(\xi) = \frac{\tau_b}{\pi} \log |1-\xi| \ ,$$

$$\xi \to 1$$

While because of the mapping $\tau(1) = \tau(-1)$ we find that near $\xi = -1$

$$u(\xi) = -\frac{\tau_b}{\pi} \log |1+\xi|$$

If we now consider the differential equation

$$u^+ - u^- = \frac{cC_J}{2} \frac{d\tau}{d\xi} \cdot \frac{d\xi}{dx}$$

which must be satisfied at $\xi = 1$ we note that because $\frac{d\xi}{dx}$ is regular near $\xi = 1$ we must have a logarithmic singularity in $\frac{d\tau}{d\xi}$ here. By considering only the singular parts of the expression we get, near $\xi = 1$,

$$\tau_b \log |1-\xi| = \frac{c}{h} C_J \frac{\pi^2}{4} (a+k) \frac{(1+k)}{1-a} \frac{d\tau}{d\xi} \ .$$

This dictates the behaviour of τ_τ near $\xi = 1$, namely

$$\tau_\tau(\xi) = \tau_b$$

$$\xi \to 1$$

$$\frac{d\tau_\tau}{d\xi}(\xi) = O(\log |1-\xi|) \ .$$

$$\xi \to 1$$

Now near $\xi = -1$ we note from the transformation

$$\frac{d\tau}{d\xi^+}\,\frac{d\xi^+}{dx} = \frac{d\tau}{d\xi^-}\,\frac{d\xi^-}{dx}$$

so that

$$\frac{d\tau}{d\xi^-} = \frac{d\tau}{d\xi^l}\,\frac{1+k}{1-a}\,\frac{-1-a}{-1+k}$$

Thus $\frac{d\tau}{d\xi^-}$ is also logarithmically infinite near $\xi = -1$.

It is of interest to analyze the physical significance of this behavior. We note in the real plane, that the flow turns through a finite angle τ_b at the trailing edge. When analyzed by linear theory this will give rise to logarithmically infinite u perturbation velocities. These velocities produce pressures being locally infinite to the same order. Now we have the dynamic boundary condition which essentially relates the curvature of the jet to the pressure difference it sustains; with the jet coefficient C_J serving as a scaling factor. Thus the pressures near the trailing edge produce an infinite curvature in the jet and this curvature, $\frac{d\tau}{dx}$, is of the same order as the pressures causing it.

This singularity in the perturbation field presents difficulties in numerical solution of the differential equation near $\xi = 1$. Fortunately this is a very weak singularity and is readily integrable so that there are simple techniques for handling it.

F. FLOW FIELDS AT INFINITY

It is useful to investigate the order of the perturbation velocities at infinity, particularly in view of the fact that the point K, corresponding to infinity downstream on the jet surface in the real plane, becomes a finite point in the ζ plane. For this purpose we consider the real flow field, adding an image singularity distribution to account for the ground plane.

We consider an unknown vorticity distribution $\gamma(x)$ defined along the airfoil and its wake, then we obtain

$$iw(z) = + \frac{1}{2\pi} \int_0^\infty \frac{\gamma(t)}{t-z}\, dt$$

We note now, for finite lifts, that $\int_0^\infty \gamma(t)dt$ exists and assume that for t large we may write $\gamma(t)$ as

$$\gamma(t) = k/t^n \qquad t > A^* \ .$$

Then

$$iw(z) = + \frac{1}{2\pi} \int_0^{A^*} \frac{\gamma(t)}{t-z}\, dt + \frac{1}{2\pi} \int_{A^*}^\infty \frac{k/t^n}{t-z}\, dt \ .$$

Now considering the velocity near the wake for $R(z) >> A^*$ we expand the first integral to write

$$\int_0^{A^*} \frac{\gamma(t)}{t-z}\, dt - \frac{1}{z} \int_0^{A^*} \frac{\gamma(t)}{1-t/z}\, dt$$

$$= \frac{1}{z} \int_0^{A^*} \gamma(t) \{1 + t/z + t^2/z^2 \ldots\}\, dt$$

$$= \frac{\Gamma^*}{z} + \frac{\Gamma_1^*}{z^2} + \frac{\Gamma_2^*}{z^3} + O(\frac{1}{z^4})$$

where $\Gamma_i^* = \int_0^{A^*} \gamma(t) t^i dt$, $\Gamma^* = \Gamma_o^*$

For the second integral we consider the function

$$-i\, w(z) = \frac{1}{z^n} \log(A^* - z) + g(z), \text{ where } g(z)$$

is a rational polynomial which must remove any singularities in v from w(z). By expanding $\frac{1}{z^n} \log(A^* - z)$ near zero we obtain

$$-iw(z) = \frac{1}{z^n} \log\,(A^* - z) - \frac{\log A^*}{z^n} + \frac{1}{A^* z^{n-1}} \cdots + \frac{1}{(n-1)A^{*n-1} z}$$

We note that this gives the analytic function implied by the second integral, namely

$$\left.\begin{array}{l} \mathcal{I}(z) = 0 \\ \mathcal{R}(z) < A^* \end{array}\right\} \qquad \left\{\begin{array}{l} u = 0 \\ v = \dfrac{1}{x^n} \log(A - x) - g(x) \end{array}\right. .$$

while for

$$\left.\begin{array}{l} \mathcal{I}(z) = 0 \\ \mathcal{R}(z) > A^* \end{array}\right\} \qquad \left\{\begin{array}{l} u = \dfrac{\pi}{x^n} \\ v = -\dfrac{1}{x^n} \log\,|A^* - x| - g(x) \end{array}\right.$$

Observing further that $u^+ - u^- = \gamma(x)$ we see that we may write the total w(z) as

$$iw(z) = \frac{\Gamma^*}{z} + \frac{1}{2(n-1)A^{*n-1}} \frac{1}{z} + \frac{b_1}{z^2} + \frac{b_2}{z^3} + \cdots .$$

We now consider the influence of an identical image vorticity distribution, situated along a line displaced vertically by 2h. This

gives $iw(z) - iw(z-2ih) = \underset{R(z)\to\infty}{b_o}\left[\frac{1}{z} - \frac{1}{z-2ih}\right] + b_1\left[\frac{1}{z^2} - \frac{1}{(z-2ih)^2}\right]$

$$+ b_3\left[\frac{1}{z^3} - \frac{1}{(z-2ih)^3}\right] + \ldots .$$

To determine v on the wake we are concerned with the real part of this expression and by expanding for $h/x < 1$ we obtain

$$v(x) = b_o \frac{4h^2}{x^3} + O\left(\frac{1}{x^5}\right)$$

Now for the vorticity $\gamma(x) = u^+ - u^-$ we consider the differential equation $u^+ - u^- = \frac{cC_J}{2}\frac{dv}{dx}$ to obtain

$$\gamma(x) = \underset{x\to\infty}{O(1/x^4)}$$

which implies that in our original assumption $\gamma(t) = k/t^n$, $t > A^*$ that $n = 4$.

We now consider the mapping derivative to obtain $v(\xi)$ near the infinities of the real plane. We have observed that for $\xi \to \infty$ we obtain the result $z = \frac{h}{(a+k)\pi}\zeta + 0\,(\log(k-\zeta))$.

so that $v(\xi) = \underset{\xi\to\infty}{O\left(\frac{1}{\xi^3}\right)}$

While near the point K we have

$$z = -\frac{h}{\pi}\log(\zeta + k) + O(\zeta)$$

so that $v(\xi) = \underset{\xi\to -k}{O\left(\frac{1}{(\log(\xi+k))^3}\right)}$

This result shows that the derivative $\frac{dv}{d\xi}$ is singular near $\xi = -k$.

A sketch, Fig. 5, of the boundary conditions for Case 1 shows the behaviour of the functions u,v.

G. CONDITIONS AT ENDPOINTS OF WAKE

1. Flow at Trailing Edge

The combination of the velocity discontinuity, and the dynamic boundary condition give us, for $\tau_b = 1$.

$$\log(\xi-1) \rightarrow \frac{c}{h} C_J \frac{\pi^2}{4} (a+k) \frac{1+k}{1-a} \frac{d\tau}{d\xi} \quad \text{near } \xi = 1$$

From this we can obtain the first term in the expansion near here

$$(\tau(\xi)-1) \frac{c}{h} C_J \frac{\pi^2}{4} (a+k) \frac{1+k}{1-a} = (\xi - 1)\{\log(\xi - 1) - 1\}$$

$$+ \text{higher order terms.}$$

2. Flow at Infinity

Considering the flow in the real z plane we see that by linear theory, the lift coefficient may be expressed

$$\frac{cC_L}{2} = -\int_0^\infty u^+(x)dx + \int_0^\infty u^-(x)dx$$

$$\frac{cC_L}{2} = \int_0^\infty \gamma(x)dx \qquad \text{where } \gamma \text{ is the vorticity.}$$

From this vorticity we obtain the v field at infinity on the wake as

$$v(x) \underset{x\rightarrow\infty}{=} \frac{2}{\pi} \frac{h^2}{x^3} \int_0^\infty \gamma(x)dx + O(1/x^5)$$

Mapping this to the corresponding flow in the ζ plane we obtain

$$v(\xi) \underset{\xi\rightarrow\infty}{\sim} \pi^2 \frac{c}{h} (a+k)^3 C_L \frac{1}{\xi^3}$$

$$v(\xi) \underset{\xi\rightarrow -k}{\sim} -\pi^2 \frac{c}{h} C_L \frac{1}{\{\log(\xi + k)\}^3}$$

H. SECOND ORDER EFFECTS

Some important overall results may be obtained by considering second order effects near the leading and trailing edges. This was exploited by Spence (Ref. 12) for the case with no ground plane, it is extended in our case.

Considering the flow in the real plane for the flat plate airfoil we obtain immediately, by considering momentum flux through a large control surface enclosing the airfoil that there is a net thrust on the device given, in coefficient form, by C_J. Now, referring to Fig. 6 we write down the equations of equilibrium for the vertical and horizontal directions, defining C_L^* as the pressure lift on the upper and lower surfaces of the airfoil and C_T as the nose thrust due to the nose singularity (this will be shown in the following paragraphs to be parallel to the airfoil chord).

$$C_T \sin\alpha + C_L^* \cos\alpha + C_J \sin(\theta+\alpha) = C_L$$

$$C_T \cos\alpha - C_L^* \sin\alpha + C_J \cos(\theta+\alpha) = C_J$$

We now eliminate C_L^* to obtain

$$C_T = C_L \sin\alpha + C_J \{\cos\alpha - \cos\alpha\cos(\theta+\alpha) - \sin\alpha\sin(\theta+\alpha)\}$$

Expanding the trigonometric functions, while neglecting terms of $O(\alpha^3)$ and above, we get

$$C_T = C_L \alpha + C_J (\theta^2/2 - \alpha^2/2)$$

To express C_T we note that if the flow near the nose in the

real plane is expressed in velocity normalized terms as $u(x) \underset{x \to o}{=} \frac{N}{x^{1/2}}$ then by applying the theorem of Blasius to a vanishingly small circle at the nose we obtain

$$C_T = \frac{2\pi N^2}{c}$$

Now by the linearity of the problem with respect to α, θ we write $N = N_\alpha \alpha + N_\theta \theta$ so that we get

$$C_T = \frac{2\pi}{c} (N_\alpha^2 \alpha^2 + 2N_\alpha N_\theta \alpha\theta + N_\theta^2 \theta^2)$$

while writing $C_L = C_{L_\alpha} \alpha + C_{L_\theta} \theta$ we obtain from the force equation

$$C_T = (C_{L_\alpha} - C_J/2)\alpha^2 + C_{L_\theta} \alpha\theta + C_J \theta^2/2 .$$

By comparing the two expressions and noting that they are identities in θ, α we obtain three equations

$$C_{L_\alpha} - C_J/2 = \frac{2\pi}{c} N_\alpha^2$$

$$C_{L_\theta} = \frac{4\pi}{c} N_\alpha N_\theta$$

$$C_J = \frac{4\pi}{c} N_\theta^2$$

By further elimination we obtain the result

$$C_{L_\theta}^2 - 2C_J C_{L_\alpha} - C_J^2$$

This is an important equation, because it implies that we are able to deduce C_{L_α} from C_{L_θ}, in other words it is necessary only to solve for the Basic Jet Angle Case (where $\alpha \equiv 0$) to infer the lift

slope with respect to angle of attack. We note also that C_{L_θ}, C_{L_α} are functions of h/c and C_J.

Considering the Basic Jet Angle Case we observe that the above result gives an exact expression for N_o, the nose source. In the discussion of the nose singularity we showed

$$u(x) \sim \frac{N_o}{2^{1/2}\pi^{3/2}} \frac{h^{1/2}}{(a+k)} \frac{1}{x^{1/2}}$$

so that

$$C_J = \frac{h}{c} \frac{2}{(a+k)^2} \frac{N_o^2}{\pi^2} \quad \text{for Case 1.}$$

I. GEOMETRICAL LINEARIZING TERM

It is clear that h/c is a significant physical parameter of all the solutions; however, because of the complicated implicit nature of the transformation, it has been convenient to work also with a, k which are also functions of h/c. At this point we introduce a fundamental geometrical term which while not readily identifiable physically results in great analytical simplification both of subsequent equations and of various limiting cases.

We recall the result

$$c/h = \frac{1-a}{(a+k)\pi} - \frac{1}{\pi} \log \frac{1+k}{a+k}$$

and the auxiliary relationship between a and k

$$(a+k) \log \frac{k+1}{k-1} = 2$$

Then noting the limiting results:

$$k \to \infty, \qquad a \to o, \qquad c/h \to \infty$$

$$k \to 1, \qquad a \to -1 - 2/\log(\frac{2}{k-1}), \qquad c/h \to 0$$

We define a new parameter G as follows:

$$G^2 = 2\pi\, c/h\, (a+k)^2 = 2(a+k)(1-a) - 2(a+k)^2 \log \frac{1+k}{a+k}$$

Here we see

$$k \to \infty, \qquad c/h \to \infty; \qquad G \to 1$$

$$k \to 1, \qquad c/h \to 0; \qquad G \to 0$$

Substituting this parameter into the expression for N_o for case 1 gives

$$N_o = \frac{\sqrt{\pi}}{2} \; G\sqrt{C_J} \quad .$$

J. CASE OF ZERO GROUND PLANE

When we put $h/c \to \infty$ we obtain the classic case treated by Spence (Ref. 2). His technique was different from that employed here, in that the problem was handled in the real plane exploiting various symmetries, anti-symmetries and inversions which are no longer valid with a ground plane. It is of interest to treat the Spence case using our techniques.

Here we have $a = 0$, $k = \infty$ and the transformation given by $z = c\zeta^2$. We see that we have the thickness solution $\tau_\tau \equiv 0$ so that thickness has no effect on the jet shape, as might be expected from a linear theory. Again from the symmetry we obtain

$$u(\xi^+) = -u(\xi^-)$$

with the dynamic condition given by

$$2u(\xi) = \frac{cC_J}{2} \frac{d\tau}{d\xi} \cdot \frac{1}{z\xi}$$

We now put $a - y'_c = y'_a$ (noting that thickness does not affect the solution) and $c = 1$ and derive, after some manipulation the integro-differential equation in the ζ plane:

$$\frac{1}{2} \frac{C_J}{4\xi} \cdot \frac{d\tau}{d\xi} = \frac{-2\xi}{\pi} \int_0^1 \frac{y'_a(t)}{(t-\xi)(t+\xi)}\, dt - \frac{2\xi}{\pi} \int_1^\infty \frac{\tau(t)}{(t-\xi)(t+\xi)}\, dt$$
$$- \frac{2}{\pi\xi} \int_0^1 y'_a(t)dt - \frac{2}{\pi\xi} \int_1^\infty \tau(t)dt$$

Transforming to the z plane gives

$$\frac{C_J}{4} \frac{d\tau}{dx} = -\frac{x^{-\frac{1}{2}}}{\pi} \int_0^1 \frac{y'_a(\eta)\eta^{\frac{1}{2}}}{\eta - x}\, d\eta - \frac{x^{-\frac{1}{2}}}{\pi} \int_1^\infty \frac{\tau(\eta)\eta^{\frac{1}{2}}}{\eta - x}\, d\eta$$

The integrals may be inverted by the general solution of the finite range Hilbert Transform (sometimes called the airfoil equation); see for example Tricomi (Ref. 13):

$$A(\xi) = \frac{1}{\pi}\int_0^1 \frac{B(x)}{x-\xi}\,dx, \qquad 0 < \xi < 1$$

$$B(\xi) = -\left(\frac{1-\xi}{\xi}\right)^{\frac{1}{2}} \frac{1}{\pi}\int_0^1 \frac{A(x)}{x-\xi}\left(\frac{x}{1-x}\right)^{\frac{1}{2}} dx + \frac{C}{\{\xi(1-\xi)\}^{\frac{1}{2}}}, \quad 0 < \xi < 1$$

If we now change the limits of these forms we obtain an alternative inversion

$$A(\xi) = \frac{\xi}{\pi}\int_1^\infty \frac{B(x)}{x}\,\frac{dx}{x-\xi}, \qquad 1 < \xi$$

$$B(\xi) = -\xi(\xi-1)^{\frac{1}{2}}\,\frac{1}{\pi}\int_1^\infty \frac{A(x)}{x}\,\frac{1}{(x-1)^{\frac{1}{2}}}\,\frac{dx}{x-\xi} + \frac{C\xi}{(\xi-1)^{\frac{1}{2}}}, \quad 1 < \xi$$

Applying this inversion, with C in the homogeneous part equal to zero we obtain, after further manipulation:

$$\tau(\xi) = \left(\frac{\xi-1}{\xi}\right)^{\frac{1}{2}} \frac{1}{\pi}\int_1^\infty \frac{C_J}{4}\,\tau'(\eta)\left(\frac{\eta}{\eta-1}\right)^{\frac{1}{2}}\frac{d\eta}{\eta-\xi}$$

$$- \frac{\xi-1}{\xi}^{\frac{1}{2}}\,\frac{1}{\pi}\int_0^1 y_a'(\eta)\left(\frac{\eta}{\eta-1}\right)^{\frac{1}{2}}\frac{d\eta}{\eta-\xi}, \qquad 1 < \xi$$

where $\tau'(\eta) = \frac{d\tau}{d\eta}$. We notice that this corresponds to Spence's Eq. 69 in Ref. 2. We further notice that for Case 1 the result $N_o = \frac{\sqrt{\pi}}{2}\sqrt{C_J}$ is given by Spence; this corresponds to G = 1, h/c = ∞ in our general expression for N_o.

K. SOLUTION OF INTEGRO-DIFFERENTIAL EQUATION

1. General

We wish to solve the equation

$$u^+ - u^- = \frac{cC_J}{2} \frac{dv}{d\xi} \cdot \frac{d\xi}{dx}, \quad 1 < \xi$$

where v is specified for $\xi^2 \leq 1$ and for $\xi < -k$. We consider first Case 1 which contains all the essential characteristics of the solution and from which the general cases easily follow. We shall approximate $v(\xi)$, $\xi > 1$ by a trapezoidal distribution defined at N values of ξ between $\xi = 1$ and $\xi = \xi_N$ with a polynomial $O(1/\xi^3)$ for $\xi > \xi_N$; the differential equation is then satisfied at points $\bar{\xi}_n$ intermediate to the locations at which v is specified. This is illustrated in Fig. 7. We call ξ_n the station points, $\bar{\xi}_n$ the control points.

2. Basic Induction Function

Considering the elementary trapezoidal v distribution of Fig. 7 we note that the analytic function $W_n(\xi) = U_n - iV_n$ satisfies the requirements enumerated below

$$W_n(\xi) = -\frac{1}{\pi}\left(V_n + \frac{V_{n+1}-V_n}{\xi_{n+1}-\xi_n}(\xi-\xi_n)\right)\log\frac{\xi-\xi_{n+1}}{\xi-\xi_n} - \frac{V_{n+1}-V_n}{\pi} - \frac{V_{n+1}+V_n}{2}\,\frac{\xi_{n+1}-\xi_n}{\xi-a}$$

a) $V_n(\xi) = V_n + \frac{V_{n+1}-V_n}{\xi_{n+1}-\xi_n}(\xi-\xi_n), \quad \xi_n < \xi < \xi_{n+1}$

b) $V_n = 0, \quad \xi < \xi_n, \quad \xi > \xi_{n+1}$

c) $W_n(\xi) = O(\frac{1}{\xi^2}), \quad \xi \to \infty$

d) $W_n(\xi) = O(\frac{1}{\xi-a}), \quad \xi \to a$

We may write $U_n(\xi)$ as:

$$\pi U_n(\xi) = V_n A_n(\xi) + V_{n+1} B_{n+1}(\xi)$$

where $$A_n(\xi) = -\log \left| \frac{\xi_{n+1}-\xi}{\xi_n-\xi} \right| \left\{ 1 + \frac{\xi_n-\xi}{\xi_{n+\eta}-\xi} \right\} + 1 + \frac{\xi_{n+1}-\xi_n}{2(\xi-a)}$$

$$B_n(\xi) = \log \left| \frac{\xi_n-\xi}{\xi_{n-1}-\xi} \right| \left\{ \frac{\xi_{n-1}-\xi}{\xi_n-\xi_{n-1}} \right\} - 1 - \frac{\xi_n-\xi_{n-1}}{2(\xi-a)}$$

3. Total Induction Function

Due to the right-hand side trapezoidal v function only, we obtain

$$\pi U(\xi) = \sum_0^N C_n(\xi)\, V_n$$

where $C_n = A_n + B_n$ and $A_o - B_N = 0$.

Now we consider an elemental distribution on the left-hand side ($-k < \xi < -1$). We note that

$$V(\xi^+) = V(\xi^-)$$

so that if we denote the corresponding point to ξ_i for $\xi_i > 1$ as ξ_i^- we obtain for the u induction

$$\pi U(\xi) = V_n A_n^-(\xi) + V_{n+1} B_{n+1}^-(\xi)$$

where $$A_n^-(\xi) = \log \left| \frac{\xi_{n+1}^- - \xi}{\xi_n^- - \xi} \right| \left\{ 1 + \frac{\xi_n^- - \xi}{\xi_{n+1}^- - \xi_n^-} \right\} - 1 - \frac{\xi_{n+1}^- - \xi_n^-}{2(\xi-a)}$$

$$B_n^-(\xi) = -\log \left| \frac{\xi_n^- - \xi}{\xi_{n-1}^- - \xi} \right| \left\{ \frac{\xi_{n-1}^- - \xi}{\xi_n^- - \xi_{n-1}^-} \right\} + 1 + \frac{\xi_{n-1}^- - \xi_n}{2(\xi-a)}$$

and hence for the left-hand side trapezoidal function we get

$$\pi U(\xi) = \sum_{0}^{N} C_n^- (\xi)\, V_n$$

where $C_n^-(\xi) = A_n^-(\xi) + B_n^-(\xi)$ and $B_o^-(\xi) = A_N^-(\xi) = 0$

Thus for the total induction due to the trapezoidal portion we have

$$\pi U(\xi) = \sum_{0}^{N} \left(C_n(\xi) + C_n^-(\xi) \right) V_n$$

We have still to consider the induction due to the v distribution between ξ_N and infinity. We do not intend satisfying the differential equation in this region, so that the exact shape is not particularly important, however, the convergence will be more rapid if the v function is a good approximation. On the right-hand side we have shown that

$$V(\xi) = O(1/\xi^3)$$
$$\xi \to \infty$$

Consequently here we use a form

$$V(\xi) = a_\tau/\xi^3 + b_\tau/\xi^5$$

with the condition $V(\xi_N) = V_N$, $V'(\xi_N) = 0$. This gives us for the induction u,

$$-\pi U_R(\xi) = a_\tau \left\{ \frac{\log|1-\xi^*|}{\xi^{*3}} + \frac{1}{\xi^{*2}} + \frac{1}{2\xi^*} - \frac{1}{2(\xi - a)} \right\}$$
$$+ b_\tau \left\{ \frac{\log|1-\xi^*|}{\xi^{*3}} + \frac{1}{\xi^{*4}} + \frac{1}{2\xi^{*3}} + \frac{1}{4\xi^*} - \frac{1}{4(\xi-a)} \right\}$$

where $\xi^* = 1 - \xi_N + \xi$

By suitable choice of a_τ, b_τ we obtain a function linear in V_N

$$\pi U_R(\xi) = V_N R(\xi)$$

On the left-hand side we have near K

$$v(\xi) = O\left(\frac{1}{(\log|\xi+k|)^3}\right)$$
$$\xi \to -k$$

We do not attempt to approximate this form too precisely, partly because unlike the right-hand side the range is finite (equal to $-k + \bar{\xi}_N$) so that errors here are small and of order $\frac{1-k}{N}$ outside the final segment, and partly because of the obvious algebraic complexity of the function. We use a simple triangular distribution having the form

$$V(\xi) = V_N \frac{\xi - \bar{\xi}_N}{-k-\bar{\xi}_N}$$

The induction is written in a form similar to that used for the elementary trapezoidal distributions to give us

$$\pi U_L(\xi) = V_N L(\xi)$$

Now we can write the total induction due to the entire v distribution as:

$$\pi U(\xi) = \sum_0^N \left(C_n(\xi) + \bar{C}_n(\xi)\right) V_n + V_N \left(R(\xi) + L(\xi)\right)$$
$$= \sum_0^N D_n(\xi)\, V_n$$

4. Slope Terms

We have the basic slope term $\frac{cC_J}{2}\pi\frac{d\xi}{dx}\frac{dv}{d\xi}$ with $\frac{d\xi}{dx}=\frac{\pi(a+k)}{h}\frac{\xi+k}{\xi-a}$. If we consider some control point $\bar{\xi}$ lying between ξ_n and ξ_{n-1} we get for the above expression, $\frac{c}{h}\frac{\pi^2}{2}(a+k)\frac{\bar{\xi}+k}{\bar{\xi}-a}\cdot C_J\frac{1}{\xi_n-\xi_{n-1}}\cdot(V_n-V_{n-1})$ which we define as $S_n^*(\bar{\xi})(V_n-V_{n-1})$.

5. Fundamental Linear Set

We may now write the differential equation as

$$\sum_0^N (D_i(\bar{\xi}^+)-D_i(\bar{\xi}^-))\,V_i = S_n^*(\bar{\xi}^+)(V_n-V_{n-1}),\quad n=1\ldots N$$

where $\xi_{n-1}<\bar{\xi}^*<\xi_n$

We now choose N points at which we wish to satisfy the equation defining these points as $\bar{\xi}_1^+$ (with $\bar{\xi}_i^-$ its left-hand transform). Now, writing $D_i(\bar{\xi}_n^+)-D_i(\bar{\xi}_n^-)=E_{in}$ and $S_n^*(\bar{\xi}_n^+)=S_n$ we obtain the linear set

$$\sum_0^N E_{in}V_i = S_n(V_n-V_{n-1}) \qquad n=1\ldots N$$

Defining again the matrix F_{ij} by

$$\begin{aligned} F_{ij} &= S_j && i=j\\ &= -S_j && j=i+1\\ &= 0 && \text{otherwise}\end{aligned}$$

yields

$$\sum_0^N (E_{in}+F_{in})V_i = 0 \qquad n=1\ldots N$$

Now we have the initial condition at the trailing edge $V_o = 1$, hence derive the set of equations:

$$(E_{in} + F_{in})\, V_i = -(E_{on} + F_{on}) \qquad n = 1 \ldots N$$

This is the final linear set of simultaneous equations which must be solved for the set V_i, being the solutions to the basic case.

III. CONVERGENCE OF THE LINEAR INTERPOLATION

A. GENERAL

In the following sections we develop a proof of the convergence of the linear interpolation used in deriving the set of linear equations which form the basis of the numerical solution. We note first that as we have assumed for $\xi^2 > 1$ a continuous approximate v distribution, having piecewise continuous derivatives, there will be no singularities of u in the range $\xi^2 > 1$. The only difficulties occur at the extremities of the v range, $\xi^2 = 1$, $\xi = -k$, $\xi = \infty$; and here the present technique is still adequate. However, we can show, through the convergence analysis, that refinements in the control point spacing can increase the convergence rate.

As a prototype of the linear interpolation scheme we analyze the case of $h/c = \infty$, and assume equidistant station and control points. While this case was not actually done in the present paper, because it would necessitate a modified program and is fully covered by Spence's Theory, it provides a valid basis for the convergence proof with greatly simplified algebra. The extension to the case of finite h/c with non-uniform station spacing follows quite readily.

B. SYMMETRICAL CASE, $h/c = \infty$

1. Basic Integro-differential Equation

Considering the Basic Jet Angle case we obtain the integro-differential equation from

$$-\frac{\pi C_J}{16}\frac{1}{\xi}\frac{dv}{d\xi} = \int_{-\infty}^{\infty}\frac{v(t)}{t-\xi}\,dt - \frac{1}{\xi}\int_{-\infty}^{\infty} v(t)\,dt, \quad \xi \geq 1$$

where $v(t) = v(-t)$

$v(t) = 0, \quad 0 < t^2 < 1$

$v(1) = 1$

$v(\xi) = O(1/\xi^2)$

$\xi \to \infty$

We then define, for brevity, a linear integral operator for the right-hand side, L , where

$$L\{v(\xi)\} \equiv \int_{-\infty}^{-1} v(t)\,\frac{dt}{t-\xi} + \int_{1}^{\infty} v(t)\,\frac{dt}{t-\xi} - \frac{1}{\xi}\int_{-\infty}^{\infty} v(t)dt$$

2. Definition of Error Function

We define $v(\xi)$ as the exact solution, and the continuous interpolation function $V(\xi)$ as the approximate solution. We note that in the interpolation and polynomial ranges we have:

$$V(\xi) = V(\xi_{n+1})\left\{\frac{\xi-\xi_n}{\xi_{n+1}-\xi_n}\right\} + V(\xi_n)\left\{\frac{\xi_{n+1}-\xi}{\xi_{n+1}-\xi_n}\right\}, \quad n = 0 \ldots N$$

$$V(\xi) = V(\xi_N)\left\{\frac{3}{\xi^{*2}} - \frac{2}{\xi^{*3}}\right\} \qquad \xi^* \geq 1$$

where $\xi^* = \xi + 1 - \xi$

For brevity we denote any function evaluated at ξ_n as $f(\xi_n) \equiv f_n$. We now define an error function in two parts, the first, $E(\xi)$, being an interpolation and polynomial having an identical functional form to $V(\xi)$, the second part being defined as $e(\xi)$ (Fig. 7). Thus

$$v(\xi) = V(\xi) + E(\xi) + e(\xi)$$

with $\quad v_n = V_n + E_n, \quad e_n = 0 \qquad n = 0 \ldots\ldots N$

Following the procedure of II.K.3 we can write the equation

$$-\frac{\pi}{16}\, C_J\, \frac{1}{\bar{\xi}_{n+1}}\, \frac{V_{n+1}-V_n}{\xi_{n+1}-\xi_n} = \mathcal{L}\left\{V(\bar{\xi}_{n+1})\right\}$$

as

$$-\frac{\pi}{16}\, C_J\, \frac{1}{\bar{\xi}_n}\, \frac{V_n-V_{n-1}}{\xi_n-\xi_{n-1}} = \sum_0^N \left\{C_i(\bar{\xi}_n)-C_i^-(\bar{\xi}_n)\right\}V_i + V_N\left\{R_1(\bar{\xi}_n)+L_1(\bar{\xi}_n)\right\}$$

$$= \sum_0^N D^*_{in}\, V_i$$

where $R_1(\xi)$, $L_1(\xi)$ correspond in form to the induction functions $R(\xi)$, $L(\xi)$ except that the former are derived for the polynomial $O(1/\xi^2)$ on both left- and right-hand sides.

We will regard the above equation as defining a linear set of equations for V_i by substituting ξ_n for $n = 1 \ldots\ldots N$ and $V_o = 1$. As before, $\xi_{n-1} < \bar{\xi}_n < \xi_n$.

We now note that we may write the mean slope of V in similar form as

$$\frac{dv}{d\xi}(\bar{\xi}_n) = \frac{v_n - v_{n-1}}{\xi_n - \xi_{n-1}} + g(\bar{\xi}_n) , \quad n = 1 \ldots . N$$

where $g(\xi)$ is an error to be discussed in the next paragraph.

3. Interpolation and Polynomial Errors

At this point we assume the control points to be taken equidistant between the station points, and that these station points are themselves equally spaced; so that we may define an internal $\Delta\xi = \xi_n - \xi_{n-1}$ for $n = 1 \ldots . N$.

From this we immediately have the result, in the region where the derivatives of v exist, that

$$\frac{dv}{d\xi}(\bar{\xi}_n) = \frac{v_n - v_{n-1}}{\Delta\xi} + O\left(\Delta\xi^2 \frac{d^3 v}{d\xi^3}\right) \qquad n = 2 \ldots . N$$

However, for the first station we note from the asymptotic analysis $v(\xi) = 1 + H(\xi-1)\{\log(\xi-1) - 1\} + O(\xi-1)$. (Here H is a bounded variable constant which will be used in further equations without implying it has the same value in different contexts.) Thus we get:

$$\frac{dv}{d\xi}(\bar{\xi}_1) = \frac{v_1 - 1}{\Delta\xi} + O(1)$$

So we may write

$$g(\bar{\xi}_n) = O(1) \qquad n = 1$$
$$= O(\Delta\xi^2) \quad n = 2 \ldots . N$$

Again we show that where the required derivatives exist

$$e(\xi) = O\left(\Delta\xi^2 \frac{d^2 v}{d\xi^2}\right) \qquad \xi_1 \leq \xi \leq \xi_N$$

while for the first station, from the asymptotic analysis

$$e(\xi) = O(\Delta\xi) \qquad 1 \leq \xi \leq \xi_1$$

To define $e(\xi)$ for $\xi > \xi_N$ we assume v to have the form

$$v = \frac{a}{\xi^2} + \frac{b}{\xi^3} + O(\frac{1}{\xi^4}) \qquad \xi \geq \xi_N$$

while in this range V and E are given by

$$\frac{V}{V_N} = \frac{E}{E_N} = \frac{3}{\xi^{*2}} - \frac{2}{\xi^{*3}}, \quad \xi^* \geq 1$$

Consequently, noting that $e(\xi_N) = 0$ we have

$$e(\xi) = O(V_N/\xi^{*2}) \qquad \xi \geq \xi_N$$

Thus we may write

$$\begin{aligned} e(\xi) &= O(\Delta\xi) && 1 \leq \xi \leq \xi_1 \\ &= O\left(\Delta\xi^2 \frac{d^2v}{d\xi^2}\right) && \xi_1 \leq \xi \leq \xi_N \\ &= O(V_n/\xi^2) && \xi_N \leq \xi \end{aligned}$$

4. Derivation of Error Matrix

If we now subtract the equations for v and V we obtain

$$\frac{-\pi C_J}{16\,\bar{\xi}_{n+1}} \left\{ \frac{E_{n+1} - E_n}{\Delta\xi} + O(1) \right\} = \sum_0^N D^*_{in} V_i + \mathcal{L}\left\{e(\bar{\xi}_{n+1})\right\}, \quad n = 0 \ldots N-1$$

We note $e(\xi) = e(-\xi)$, and using the bounds derived above, define e for $\xi \geq 1$ in two parts, defined for $\xi \leq \xi_N$ and $\xi \geq \xi$. Thus we have $e = e_1 + e_2$ with $|e_1| \leq \Delta\xi f(\xi)$, $1 \leq \xi \leq \xi_N$ where $f(1) = 0$;

$f(\xi) = 0$ for $\xi \geq \xi_N$ and $f(\xi)$ is continuous and bounded for $1 \leq \xi \leq \xi_N$.

For e_2 we use the inequality

$$|e_2| \leq K' f_T(\xi^*) - K' \left\{ \frac{1}{\xi^{*2}} - \frac{1}{\xi^{*3}} \right\}$$

where K' is a constant, $O(V_n)$.

Now, applying the integral operator gives

$$\mathcal{L}\{f_T(\xi)\} = \int_{-\xi_N}^{-1} f(t) \frac{dt}{t-\xi} + \int_{1}^{\xi_N} f(t) \frac{dt}{t-\xi} - \frac{1}{\xi} \int_{-\xi_N}^{\xi_N} f(t)dt$$

where because $f(1) = f(\xi_N) = 0$ and $f(\xi)$ is bounded we get

$$\mathcal{L}\{f(\xi)\} = O(1) \qquad \xi \geq 1 \ .$$

For the outer portion, e_2, we consider

$$\mathcal{L}\{f_T(\xi)\} = \int_{-\infty}^{-\xi_N} \frac{f_T(t)}{t-\xi} dt - \frac{1}{\xi} \int_{-\infty}^{-\xi_N} f_T(t)dt + \int_{\xi_N}^{\infty} \frac{f_T(t)}{t-\xi} dt - \frac{1}{\xi} \int_{\xi_N}^{\infty} f_T(t)dt$$

For $1 \leq \xi \leq \xi_N$ only the latter two terms of the expression are significant and writing out these terms we get

$$\frac{1}{\xi^{*2}} \log|1-\xi^*| + \frac{1}{\xi^*} + \frac{1}{2} - \frac{1}{\xi} - \frac{1}{\xi^{*3}} \log|1-\xi^*| - \frac{1}{\xi^{*2}} - \frac{1}{2\xi^*} - \frac{1}{3} - \frac{1}{2\xi}$$

This has a maximum near $\xi^* = 1$ which is bounded and $O(1)$ so that we may write

$$\mathcal{L}\{e_2\} = O(K') = O(V_N)$$

Thus we have the two results

$$\mathcal{L}\{e_1\} = O(\Delta\xi)$$

$$\mathcal{L}\{e_2\} = O(V_n)$$

If we select ξ_N such that $v_n = O(\Delta\xi)$ we can assert $\mathcal{L}\{e\} = O(\Delta\xi)$. However for this proof we can use a cruder bound and state

$$\mathcal{L}\{e\} = O(1)$$

We now write the equations defining E_i as

$$\sum_0^N \frac{B_{in}}{\Delta\xi} E_i + O(1) = \sum_0^N D^*_{in} E_i + O(1), \quad n = 1 \ldots N$$

$$E_o = 0 .$$

Where $B_{ij} = -\frac{\pi}{16} C_J \frac{1}{\xi_j}$ $\quad i = j$

$= -B_{ij}$ $\quad j = i - 1$

$= 0$ $\quad$ otherwise

5. Determination of the Order of E_i

Now because $E_o = 0$ we can drop the terms B_{oj}, D^*_{oj} and thus obtain a linear set having N equations and N unknowns. For conciseness we define the various elements in matrix form so that

$\tilde{B}$ has elements B_{ij} $\quad$ i, j = 1.....N

$\tilde{D}$ has elements D^{*}_{ij} $\quad$ i, j = 1.....N

where i indicates the column suffix.

We define the column error vector, and column unit vector as

$\tilde{E}$ has elements E_j $\quad$ j = 1.....N

$\tilde{1}$ has elements $1_j = 1$ $\quad$ j = 1.....N

We then write the matrix equation

$$(\tilde{B} - \Delta\xi\tilde{D})\,\tilde{E} = \Delta\xi H\tilde{1}$$

We now consider the order of magnitude of the elements of the two matrices. It is evident that the elements of B are O(1) and that the determinant is non-zero so that an inverse exists. The elements of this inverse are O(1).

For $\tilde{D}$ we consider a typical element, given by $D_{ij} = C_i(\bar{\xi}_j) + C_i^{-}(\bar{\xi}_j)$ for $i < N$, where $C_i(\bar{\xi}_j) =$

$$-\left\{1 + \frac{\bar{\xi}_i - \bar{\xi}_j}{\Delta\xi}\right\} \log\left|1 + \frac{\Delta\xi}{\xi_i - \bar{\xi}_j}\right| + \frac{\xi_{i-1} - \bar{\xi}_j}{\Delta\xi} \log\left|1 + \frac{\Delta\xi}{\xi_{i-1} - \bar{\xi}_j}\right| - \frac{\Delta\xi}{\bar{\xi}_j}$$

while $C_i^{-}(\xi_j) = O(\Delta\xi)$ because $|\bar{\xi}_j| \geq 2$, all j.

Now we observe that for the control points selected

$$C_i(\bar{\xi}_j) = -\{1 + i - j + \tfrac{1}{2}\} \log\left|1 + \frac{1}{i-j+\frac{1}{2}}\right| + \{i-j+\tfrac{1}{2}\} \log\left|1 + \frac{1}{i-j-\frac{1}{2}}\right| - \frac{1}{j-\frac{1}{2}}$$

This shows us that

$$C_i(\bar{\xi}_j) = O(1) \qquad i = j,\ j = i \pm 1$$

$$C_i(\bar{\xi}_j) = O(\Delta\xi) \qquad \text{otherwise}$$

Thus we may state that the elements of D are O(1).

We now assume $\tilde{E}$ is expanded into a series of column vectors of descending magnitude

$$\tilde{E} = \tilde{E}^{(o)} + \Delta\xi\tilde{E}^{(1)} + \Delta\xi^2\tilde{E}^{(2)} + \cdots\cdots$$

where $\tilde{E}^{(i)}$ represent column vectors having elements O(1).

Now substituting to the vector equation we get

$$(\tilde{B} - \Delta\xi\tilde{D})(\tilde{E}^{(o)} + \Delta\xi\tilde{E}^{(1)} + \Delta\xi^2\tilde{E}^{(2)} + \cdots\cdot) = \Delta\xi H\tilde{1}$$

Then collecting terms of equal magnitude we get

$$\tilde{B}\,\tilde{E}^{(o)} = 0$$

$$-\tilde{D}\,\tilde{E}^{(o)} + \tilde{B}\,\tilde{E}^{(1)} = H\,\tilde{1}$$

We note $\tilde{B}^{-1}$ exists so that $\tilde{E}^{(o)} \equiv 0$ and then from the second equation obtain $\tilde{E}^{(1)}$, having elements O(1).

This completes the proof that, for ξ_N fixed and O(1), as $\Delta\xi \to 0$, we have the error vector

$$E = O(\Delta\xi)\,\tilde{1}$$

C. GENERAL CASE, h/c FINITE

For this case we generalize to the problem actually solved by numerical techniques. Here we have the added generality of non-uniform station spacing and unsymmetrical left- and right-hand v distribution. The non-uniformity of station spacing is readily handled by considering terms $O(\Delta\xi_{max})$ where $\Delta\xi_{max}$ is the maximum spacing. We choose control points by the condition $\bar{\xi}_n^- = \frac{1}{2}(\xi_n^- + \xi_{n-1}^-)$ so that $\bar{\xi}_n^+$ is determined by the mapping $\xi^+ \rightarrow \xi^-$. While this implies that $\bar{\xi}_n^+$ is no longer equidistant to its adjacent control points, the fact that $d\xi^+/d\xi^-$ is bounded for all $\xi^+ > 1$ gives us $\xi_n^+ < \bar{\xi}_n^+ < \xi_{n+1}^+$, so that again all the elements of $\tilde{D}$ are O(1).

For the continuous portion of the V curve we define

$$V(\xi) = \frac{V_N}{2} \left\{ 5/\xi^{*3} - 3/\xi^{*5} \right\} \qquad \xi \geq \xi_N$$

$$V(\xi) = V_N \frac{k+\xi}{k+\xi_N^-} \qquad -k \leq \xi \leq \xi_N^-$$

While the appropriate linear integral operator becomes

$$\mathcal{L}\{v(\xi)\} = \int_{-k}^{-1} v(t) \frac{1-\delta(t-a)}{t-\xi}\, dt + \int_{1}^{\infty} v(t) \frac{1-\delta(t-a)}{t-\xi}\, dt - \frac{1}{\xi - a} \int_{-k}^{\infty} v(t)\, dt$$

Proceeding in a manner analogous to that for the symmetrical case we can show $E_i = O(\Delta\xi_{max})$.

D. IMPROVEMENT OF CONVERGENCE RATE

The above analysis shows clearly that the convergence of the linear interpolation technique is dominated by conditions at the extremities of the v distribution.

Near $\xi^2 = 1$ the order of the error function $e(\xi)$ is changed from $\Delta\xi^2$ to $\Delta\xi$ by the logarithmic term. This degradation in convergence can be partly remedied by suitable choice of the first control point. In fact, if we choose $\xi_1 = 1 + \frac{\xi_2 - 1}{e^*}$ (where $e^* = e$, the exponential) we find

$$\frac{dv}{d\xi}(\xi_1) = \frac{v_1 - 1}{\Delta\xi} + O(\Delta\xi \log \Delta\xi)$$

$$\text{and } e(\xi) = O(\Delta\xi^2 \log \Delta\xi) \qquad 1 \leqslant \xi \leqslant \xi_1$$

The other major factor relating to convergence is the accuracy of the polynomial defined for $\xi > \xi_N$. This can be improved by increasing ξ_N, although this analysis indicates that the improvement would not become significant until $V_n = O(\Delta\xi_{max})$, which condition will occur when $\Delta\xi_{max} = O(1/\xi_N{}^3)$. A more effective technique would be to relate this polynomial linearly to V_N and V_{N-1} by matching both ordinate and slope to the linear interpolation at ξ_N. Evidently more terms can be added to the polynomial and it may be thus linked to more of the preceding values of V.

An alternative iterative procedure is to evaluate C_{L_θ} by the present method, to use this value to establish the constant in the expression $V(\xi) \underset{\xi \to \infty}{=} A/\xi^3$ and hence to obtain an excellent approximation to the leading term of the polynomial for the second improved

solution.

We note that an indication of optimum station point spacing in the linear interpolation range is provided by the expression $e(\xi) = O(\Delta\xi^2 \frac{d^2v}{d\xi^2})$: this shows that station points should be spaced more closely in the regions of high curvature, as is evident intuitively.

In practice the accuracy of the v distribution for large ξ is not of great significance. For the case of $N_o = \int_{-\infty}^{\infty} v(t)\,dt$ where we might expect it to be important we already have the exact result derived by other means, and in the case of C_{L_W} which is proportional to $\int_{-\infty}^{\infty} K(t)\,v(t)\,dt$ we have shown that the wakelift kernel decays rapidly for $\xi >> 1$ so that only the v behavior for small ξ need be accurately determined.

IV. EVALUATION OF FORCE COEFFICIENTS

A. DECOMPOSITION OF LIFT INTEGRALS

For the basic case we have $\alpha = 0$ and need not thus consider the contribution of the nose source to lift. By integrating the pressure coefficient on the upper and lower surfaces in the real plane we obtain

$$-cC_{L_B} = \int_0^c 2u^+(x)dx - \int_0^c 2u^-(x)dx$$

for the pressure contribution to the lift. Now transforming to the ζ plane removes the ambiguity in u and we get

$$-cC_{L_B} = \frac{2h}{\pi(a+k)}\int_a^1 u(\xi)\,\frac{\xi-a}{\xi+k}\,d\xi - \frac{2h}{\pi(a+k)}\int_{-1}^a u(\xi)\,\frac{\xi-a}{\xi+k}\,d\xi$$

$$\frac{\pi}{2}\,\frac{c}{h}\,(a+k)\,C_{L_B} = \int_{-1}^1 u(\xi)\,\frac{\xi-a}{\xi+k}\,d\xi$$

We note that $u(\xi)$ is singular at ± 1 and a and that we may write it in two parts, separating the polar and logarithmic singularities as

$$u(\xi) = \frac{N_o}{\pi(\xi-a)} + \frac{1}{\pi}\int_{-\infty}^{\infty} \frac{v(t)}{t-\xi}\,dt$$

We call the u component due to N_o the nose flow, and the lift associated with it the nose lift; while because v in the second integral is zero everywhere except the wake, we define the force contribution due to it as the wake lift. Then, calling the nose lift C_{L_N} we get

$$\frac{\pi}{2}\frac{c}{h}(a+k)\,C_{L_N} = \frac{N_o}{\pi}\int_{-1}^{+1}\frac{1}{(\xi-a)}\,\frac{(\xi-a)}{(\xi+k)}\,d\xi$$

$$= \frac{N_o}{\pi}\log\,\frac{k+1}{k-1}$$

Now introducing the term G and the expression for N_o we get

$$C_{L_N} = \frac{4}{\sqrt{\pi}}\,\frac{\sqrt{C_J}}{G}$$

a particularly simple expression which clearly illustrates the limiting behaviour of C_{L_N} as h/c varies.

For the wake lift, designated C_{L_W} we have the expression

$$\frac{\pi^2}{2}\frac{c}{h}(a+k)\,C_{L_W} = \int_{-1}^{+1}\int_{-\infty}^{+\infty}\frac{v(t)(\xi-a)}{(\xi-t)(\xi+k)}\,dt\,d\xi$$

$$= \int_{-\infty}^{+\infty} v(t)\left\{\frac{a-t}{k+t}\,\log\frac{t-1}{t+1} - \frac{2}{k+t}\right\}dt$$

We write this as

$$\frac{\pi^2}{4}\,\frac{G^2}{a+k}\,C_{L_W} = \int_{-\infty}^{+\infty} v(t)K(a,t)dt = \int_{-k}^{-1} v(t)K(a,t)dt + \int_{1}^{\infty} v(t)K(a,t)dt$$

defining a lift kernel K(a,t).

The lift kernel has certain desirable properties; it contains only logarithmic singularities, and these at the inner extremities of its range and, more significantly, is integrable itself, which may be seen by noting

$$K(a,t) \underset{t \to \infty}{=} O(\frac{1}{t^2}) \text{ and } K(a,-k) = \log \frac{k+1}{k-1}$$

Because of this we are able to calculate the value of C_{L_W} as $C_J \to \infty$. In this case we have $v(t) \to 1$ and consequently

$$\lim_{C_J \to \infty} \left(\frac{\pi G^2 C_{L_W}}{4(a+k)} \right) = \int_{-k}^{-1} K(a,t)dt + \int_{1}^{\infty} K(a,t)dt$$

The evaluation of this integral is discussed in the following section.

From the above decomposition, and adding the jet momentum lift, we obtain the result (for $\theta = \tau_{bl} = 1$).

$$C_L = C_{L_N} + C_{L_W} + C_J$$

B. INTEGRATION OF LIFT KERNEL

We consider the left- and right-hand parts of the integral:

$$K_L = \int_{-k}^{1} K(a,t)dt \ , \quad K_R = \int_{1}^{\infty} K(a,t)dt$$

In the appendix we show

$$K_L = (a+k)\left[B_1\left(\frac{k-1}{k+1}\right) - B_1(1)\right] + 2\log 2 + (k-1)\log(k-1) - (k+1)\log(k+1)$$

$$K_R = (a+k)\left[B_1(1) - B_1\left(\frac{k-1}{k+1}\right)\right] - 2\log 2 + 2 + 2\log(k+1)$$

where the function $B_1(x)$ is defined in the appendix.

From this we show

$$\lim_{C_J \to \infty} \left(\frac{\pi G^2}{4(a+k)} \ C_{L_W}\right) = 2 + (k-1)\log\frac{k-1}{k+1}$$

$$= 2\,\frac{a+1}{a+k}$$

$$\lim_{C_J \to \infty} C_{L_W} = \frac{8(1+a)}{\pi G^2}$$

$$- 8/\pi \quad \text{for} \quad G \to 1$$

For $G \to 0$ we require the limit $\frac{1+a}{G^2}$ as $G \to 0$.

$$G^2/(1+a) = \frac{a+k}{1+a}\left[2(1-a) - 2(a+k)\log\frac{1+k}{a+k}\right]$$

Now as $G \to 0$, $\frac{a+k}{1+a} \to 1$ so we have $G^2/(1+a) \to 4$.

Consequently

$$\lim_{C_J \to \infty} C_{L_W} = \frac{2}{\pi} \quad \text{for} \quad G \to 0$$

On the other hand, for C_J finite but $G \to 0$ we have another limit which can be evaluated as follows:

$$\frac{\pi G^2}{4(a+k)} C_{L_W} = \int_{-k}^{-1} v(t)K(a,t)dt + \int_{1}^{\infty} v(t)K(a,t)dt$$

We note

$$\int_{-k}^{-1} v(t)dt > 0 \qquad \text{and} \qquad \int_{-\infty}^{\infty} v(t)dt = N_o$$

$$\int_{1}^{\infty} v(t)dt > 0$$

Consequently $\int_{1}^{\infty} v(t)dt < N_o$, $\int_{-k}^{-1} v(t)dt < N_o$

Now considering the second integral defining C_{L_W}

$$I_2 = \int_{1}^{\infty} v(t)K(a,t)dt$$

$$= \int_{1}^{1+\nu} K v\, dt + \int_{1+\nu}^{\infty} K v\, dt$$

where $\nu = \int_{1}^{\infty} v dt$

$$I_2 = \int_{1}^{1+\nu} K dt - \int_{1}^{1+\nu} K(1-v)dt + \int_{1+\nu}^{\infty} K v\, dt$$

$$I_2 < \int_{1}^{1+\nu} K dt - K(a,1+\nu)\left\{\int_{1}^{1+\nu} (1-v)dt - \int_{1+\nu}^{\infty} v dt\right\}$$

because K is monotonic decreasing. Thus

$$I_2 < \int_{1}^{1+\nu} K dt$$

Similarly we show

$$I_1 < \int_{-1}^{-1-\mu} K dt \qquad \text{with} \qquad \mu = \int_{-k}^{-1} v dt$$

so $$\frac{\pi G^2}{4(a+k)} C_{L_W} < \int_{-1}^{-1-\mu} K dt + \int_{1}^{1+\nu} K dt$$

and ν , $\mu < N_o$

Now $$N_o = \frac{\sqrt{\pi}}{2} G \sqrt{C_J}$$

and $$\frac{G^2}{(a+k)} \underset{G \to 0}{\to} 4$$

So finally

$$C_{L_W} \underset{G \to 0}{\to} 0 \qquad \text{for } C_J \text{ finite}$$

C. LIFT CURVES FOR LOW C_J

We can utilize the relationship between C_{L_θ} and C_{L_α} to derive results for small C_J. We have

$$C_{L_\theta}^2 = 2C_J C_{L_\alpha} - C_J^2$$

where $C_{L_\alpha} = C_{L_\alpha}(h/c, C_J)$.

Then $$\lim_{C_J \to 0} \left(\frac{C_{L_\theta}^2}{C_J} \right) = 2 C_{L_\alpha}(h/c, 0).$$

The values of C_{L_α} as functions of h/c are given by Tani (Ref. 14); using these as a basis we construct the curves of Fig. 14; it will be seen that the computed points fit excellently, even up to jet coefficients of one half.

V. NUMERICAL SOLUTION

A. GENERAL

The fundamental linear matrix developed in II.K.5 was generated and the equations solved on the IBM 7094 computer. In addition, the various lift integrals were evaluated numerically.

The programming involved numerous difficulties, both in retaining accuracy in developing the matrix elements, and in accounting for the severe scaling difference between the right- and left-hand side. These were overcome by various strategems involved in grouping terms and redefining coordinates to preserve comparative magnitudes. These techniques are not of interest in this paper and so a broad discussion of procedures only is given.

The final program, consisting of a 16 point solution for the two parameter family with 10 values of c/h and 6 of C_J takes about 120 seconds. The actual execution time for a c/h, C_J pair point is about .75 seconds.

B. CHOICE OF CONTROL POINTS

We specifically avoid attempting to choose a control point at either the trailing edge or infinity for obvious reasons. However, it is desirable to space control points more closely in these areas because the curvature of the v function is more intense here. To this end we define the station points at which V_i is determined on the left-hand distribution by using the familiar circular mapping, i.e.,

$$\xi_i^- = -1 + \frac{1-k}{2}\left(1 - \cos\frac{\pi i}{N+1}\right) \qquad i = 0 \ldots N$$

We define the control points (at which the equation is to be satisfied) by

$$\bar{\xi}_i^- = \left(\xi_{i-1}^- + \xi_i^-\right)\frac{1}{2}$$

Then ξ_i^+, $\bar{\xi}_i^+$ are defined by the transcendental equation below, developed from the basic mapping of Eq. 1.

$$\frac{e^{\frac{\xi^+-a}{a+k}}}{\xi^+ + k} = \frac{e^{\frac{\xi^--a}{a+k}}}{\xi^- + k}$$

It was found necessary, for the low values of h/c and high C_J to choose a few station points closer to K than given by the circular mapping. This is easily accomplished by redefining the points ξ_N^-, ξ_{N-1}^- ... , because the basic program is written for a completely arbitrary selection of station and control points.

C. CONVERGENCE CONTROL

The solutions V_i to the linear equations generate a trapezoid which approximates the continuous V curve. However, from considerations of the nose flow we have an exact result for $N_o = \int V(\xi)d\xi$. As a consequence of this, an excellent check of the convergence and accuracy is the correlation of the computed N_o with the exact value. These are shown on Fig. 8. It will be seen that the correlation is excellent with some small discrepancies for the high jet coefficients, the error here being due to the relatively slow rate of decay of V with ξ so that the numerical procedure does not accurately give the $V(\xi)$ curve for high ξ. In other words the station points do not extend far enough. This can easily be remedied by reselecting points. However, because of limitations on computer time, it was decided to use a single station point layout for all C_J, h/c combinations; which is evidently not optimum in the extreme cases of these parameters.

Some computer experiments were conducted, varying the number of station points from 8 to 16 to 32. It was found that 16 represented an optimum of computer time and accuracy required, although this is evidently an arbitrary criterion. As an indication of the computer solutions generated, a few typical cases are shown in Figs. 9 and 10.

VI. RESULTS: CORRELATION WITH THEORY AND EXPERIMENT

A. BASIC LIFT CURVES

In IV.A we show that the lift coefficient for the Basic Case may be written as three components. Evidently because of the linearity, this is also the lift slope for this case. Thus

$$C_{L_\theta} = C_{L_N} + C_{L_w} + C_J$$

Of the three components, only C_{L_w} need be calculated by computer techniques; the other two having exact explicit representations. Thus our attention is focussed on C_{L_w} which is shown in Fig. 11. As discussed in the previous section numerical inaccuracies are introduced by poorly balanced station point selection. A measure of the inaccuracy is given by the correlation of the exact and computed nose source. In Fig. 11 an approximate correction (shown dashed) is made by scaling C_{L_w} in the ratio of the two values of the nose source; except for $C_J = 10$ this is a very small correction. It is evident from Figs. 8, 9, 10 that the station point selection for $C_J \geq 10$ should be modified, although even with the existing arrangement the percentage error is small because in this range $C_{L_w} << C_{L_N}, C_J$.

The corresponding C_{L_w} for $G = 1$ is extracted from Spence (Ref. 2) and shown; it will be seen that the correlation is excellent.

As a more direct representation C_{L_θ} and C_{L_α} for different values of h/c and C_J are shown in Fig. 12 with Spence's curve (Ref. 2) serving as a base line. In Ref. 2 the author discusses the

good correlation with experiment for his linearized theory, so our correspondence with his theoretical results may be interpreted as an experimental verification.

For the lower h/c values there is little experimental information except for a set of results quoted by Huggett in a paper (Ref. 8) in which he discusses wake blockage.

B. LIFT CURVES AT LOW h/c: WAKE BLOCKAGE

1. General

At low values of h/c the results of Ref. 8 show an apparent independence of G to h/c for low C_J followed by a lift behaviour analogous to the stall, where the lift slope abruptly reduces. Experimental work in the above paper showed clearly that this occurred when the jet impinged on the floor, causing part of the jet to flow forward and over the leading edge of the airfoil. Beyond this point the airfoil reached a plateau of its pressure lift, which then remained substantially constant for higher blowing coefficients, the increase in total lift being essentially due only to the increased jet momentum. This phenomenon is known as wake blockage.

Huggett observed that the maximum pressure lift achieved appeared to be essentially independent of jet angle or coefficient and to be related only to h/c. (It may be noted here that this observation is based only on the performance at two jet angles.) He developed a simple theory, assuming a uniform vorticity on the airfoil, and entirely neglecting wake vorticity, which gave good experimental correlation with the limited test points. However, this agreement would seem somewhat fortuitous. In the first place, completely neglecting the strong jet wake seems unacceptable; secondly the assumption of uniform vorticity on the airfoil is evidently impossible in an attached flow and assumptions that this represents a separated flow with uniform pressure on the airfoil make his inviscid potential analysis most questionable.

A model proposed by Williams (Ref. 9) removes the objections of unrealistic vorticity distribution. By an exact conformal mapping technique he finds the pressure lift on the horizontal portion of an airfoil with a deflected flap extending to the ground plane. Because of mathematical complexity he computes the results only for a flap angle of 90°. This may be expected to give an approximation of the inviscid flow for $G \to \infty$. However, the tests referred to in Ref. 8 indicate blockage in some cases at $C_J = .8$ and do not include jet coefficients above 10; while the theory of the present paper shows that even for jet coefficients of 10 there is considerable jet curvature which is neglected in Ref. 9. The blockage curve of Williams fits the experiment about as well as Huggett's theory.

It may be noted that any attempt to define blockage by considering experimental lift curves suffers the usual arbitrariness in the decision of the point at which the blockage type flow commences particularly if changes in lift coefficient are used as the only indicator.

The theory developed in this paper is essentially linear, thus it cannot be reasonably expected to make much sense for a non-linear viscous phenomenon. Nonetheless it is possible to develop an extension to the theory which gives:

(a) limits to the applicability of linear theory

(b) fairly good theoretical predictions of blockage and reasonable correlation with observed results.

2. Wake Blockage Theory

We define wake blockage to occur when there is zero net mass

flux between the lower surface of the airfoil and the ground plane. Evidently this occurs when the dividing streamline far forward is depressed by an amount h, or, what is the same thing, the jet reaches a height h below the airfoil at infinity.

We can write the deflection of the jet h_J for a finite angle θ,

$$h_J = \theta \int_1^\infty v(x)dx$$

$$= \theta \int_1^\infty v(\xi) \frac{h}{\pi(a+k)} \frac{\xi-a}{\xi+k} d\xi$$

For low values of h/c

$$k = 1 + \ell$$

$$a = -1 + 1/\log \ell/2$$

so that

$$\frac{\xi-a}{\xi+k} = 1 + \frac{1}{\xi+1} \frac{1}{\log \ell/2} + O\left(\frac{1}{(\xi+1)^2}\right)$$

Now we note for $h/c = 1.18$, $\ell = 10^{-2}$ and assume as an approximation $\frac{\xi-a}{\xi+k} \sim 1$, so that

$$h_J \sim \frac{\theta h}{\pi(a+k)} \int_1^\infty v(\xi)d\xi$$

Again we note $\int_{-k}^{-1} v(\xi)d\xi + \int_1^\infty v(\xi)d\xi = N_o$ but that $\int_{-k}^{-1} v(\xi)d\xi = O(\ell)$ so that we finally write

$$h_J = \frac{\theta h}{\pi(a+k)} N_o$$

$$\frac{h_J}{h} = \frac{\theta}{\sqrt{2}} \sqrt{\frac{cC_J}{h}}$$

This expression is of some interest, illustrating the constraint on θ, C_J, c/h for our linear theory to hold; which is implied by $h_J/h < 1$. Again it shows that at low heights a proper jet coefficient is one based on height, not chord; or that the conditions of validity of the theory are

$$\frac{\theta}{\sqrt{2}} \sqrt{C_{J_h}} < 1$$

where $C_{J_h} = \frac{\rho_J V_J^2}{\frac{1}{2}\rho U^2 h}$.

We continue along these lines, assuming blockage to occur when $\frac{\theta}{\sqrt{2}} \sqrt{\frac{c}{h} C_J} = B_h$, where B_h is a constant of order 1. Defining C_{L_p} as the pressure lift on the airfoil (at $a \equiv 0$) we get

$$C_{L_p} = (C_{L_w} + C_{L_N})\theta$$

$$= B_h \left\{ \frac{4}{\sqrt{\pi}} \frac{\sqrt{C_J}}{G} + C_{L_w} \right\} \sqrt{\frac{2h}{c}} \frac{1}{\sqrt{C_J}}$$

$$= B_h \sqrt{\frac{2h}{c}} \left\{ \frac{4}{G\sqrt{\pi}} + \frac{C_{L_w}}{\sqrt{C_J}} \right\}$$

We observe that this theoretical expression approximately predicts the observations of Huggett in that it is independent of jet angle θ and only weakly dependent on C_J (for low C_J we have $C_{L_w} / \sqrt{C_J}$ = constant).

The three different blockage predictions are plotted in Fig. 13. It should be pointed out that the actual 'meaning' of blockage is somewhat different in the three theories. For those of Huggett and Williams C_{L_p} should represent the maximum pressure lift carried by the airfoil. For the present paper, it corresponds to the C_{L_p} at which (according to linear theory) there is no net flow under the airfoil. Thus for our case it represents, in some sense, an upper limit of applicability of the linear approach, assuming that the inviscid approach still applies, i.e., that there has been no nose or trailing edge separation.

The test points as reported by Huggett are shown on the figure. These points are open to some latitude in determination from the experiments because while the tests show a fairly distinct point of departure of C_{L_p} from the linear curves there is subsequently a rather slow increase of C_{L_p} until $C_{L_{p_{max}}}$ occurs. In other words, in airfoil terminology the jet flap airfoil tested behaves rather like a thin airfoil, showing an early divergence from the theoretical lift curve occurring substantially before $C_{L_{max}}$. Thus we infer blockage to have occurred when the airfoil reaches its maximum C_{L_p} instead of by direct measurement of mass flow. A better test of the linear predictions might be obtained by actually integrating the velocity profile beneath the airfoil to determine the blockage point. It should also be noted that some means of removing the wall boundary layer, for example, a moving ground plane, might be expected to give different experimental blockage levels.

In view of these factors, associated primarily with viscous

and nonlinear effects, no close correlation can be expected between the various blockage theories and the test results. In the range of h/c between .5 and 1.5 all theories are of approximately the same order of magnitude. It will be seen from Fig. 13 that, in spite of its theoretical weaknesses that of Huggett appears the best. However a better judgment could be made if more tests, particularly in the high range of h/c and C_J, were available and if a more direct measurement of blockage were made.

Fig. 14 shows the tests reported by Huggett plotted in comparison with the present theory. It must immediately be pointed out that these tests were conducted at large jet angles (31.4^o and 58.1^o) so that the linear theory cannot be expected to fit very closely. In addition the potential effects of finite thickness are not considered. We note that in general a reasonable correlation is obtained, although there is an unaccounted inconsistency in the fact that the results for $\theta = 31.4^o$ fall below linear theory while those for $\theta = 58.1^o$ are somewhat above the predicted values. We note here that there are two potential effects: that of finite thickness and that of non-linear jet theory, which were not taken into account. It is possible that these might regularize the situation. We note, by consideration of the case of a simple flap, that the linear theory for this case overestimates the lift evaluated by exact techniques. For the thickness case we note two effects qualitatively, the thickness itself causing a negative lift at zero lift but increasing the lift curve slope.

A striking effect is the reduction in lift with reduction in h/c in the tests and the opposite behavior in the theory. This is

evidently due to the early blockage in the experiments at low h/c. These experiments show negligible difference in lift with h/c for low C_J, while the theory indicates that this difference is indeed small. When blockage commences the lower h/c values are affected first, thus causing the apparent anomaly. Blockage values predicted by linear theory with $B_h = 1$ are shown on the $\theta = 58.1^o$ curve. It will be recalled that $B_h = 1$ implies an upper limit of the onset of blockage and is not expected to predict the actual blockage C_L. It will be seen from Fig. 14 that there is however fairly good correlation.

Blockage limits for the case $\theta = 31.4^o$ do not define the $C_{L_{pmax}}$ as clearly as in the first case, as may be seen by inspection of the blockage curve Fig. 13. However they provide an upper bound again so do not introduce inconsistencies, but merely indicate that this bound is rather a crude one. In any case it may be said that the experiments are not precise enough and the linear theory extended too far beyond its range to rationally pursue the discussion in any further detail.

VII. THICKNESS AND CAMBER CASES

A. CAMBER

1. Basic Solution

We consider as the basic solution the case of a simple flap-like discontinuity in v at x_f on the airfoil. The leading portion of the airfoil is at $\alpha = 0$ and there is zero jet angle relative to the trailing edge. Thus we obtain boundary conditions in the ζ plane as shown in Fig. 16.

We observe that those conditions are identical to those for the basic case, with the addition of the v distributions on the airfoil itself.

For the right-hand side we obtain the induction

$$\pi U(\xi) = \log\left(\frac{\xi-1}{\xi-\xi_f^+}\right) + \frac{1-\xi_f^+}{\xi-a}$$

and define $M(\xi)$ as $\pi U(\xi)$.

Similarly for the left-hand side we define

$$M^-(\xi) = \pi U(\xi) = \log\left|\frac{\xi+1}{\xi-\xi_f^-}\right| + \frac{\xi_f^-+1}{\xi-a}$$

Then we define the term corresponding to $u^+ - u^-$ as

$$N_i = M(\bar{\xi}_i^+) + M^-(\bar{\xi}_j^+) - M(\bar{\xi}_i^-) - M^-(\bar{\xi}_i^-) \qquad i = 1 \ldots N$$

Now we add this to the final set of linear equations developed in II.K.5. to give the new set

$$\sum_{i=1}^{N} (E_{in}+F_{in})V_i = -(E_{on}+F_{on}+N_n) \qquad n = 1 \ldots N$$

The solution of this set yields the required V_i.

2. Lift Coefficient

As before the lift coefficient contains the terms C_{L_N} and C_{L_w} which are evaluated exactly as previously. We have an additional term C_{L_c} given by

$$\frac{\pi}{2}\frac{c}{h}(a+k)\,C_{L_c} = \int_{-1}^{+1} \frac{\xi - a}{(\xi - t)(\xi + k)}\,dt d\xi + \int_{-1}^{1}\int_{\xi_f}^{1} \frac{\xi - a}{(\xi - t)(\xi + k)}\,dt d\xi$$

$$= \int_{-1}^{\xi_f^-} K(a,t)dt + \int_{\xi_f^+}^{1} K(a,t)dt$$

This is integrated, as shown in the Appendix where I(A,B) is defined to give

$$\frac{\pi}{2}\frac{c}{h}(a+k)\,C_{L_c} = I(\xi_f^-, -1) + I(1, \xi_f^+)$$

Thus for flap deflection δ_f we have

$$C_{L_{\delta_f}} = C_{L_N} + C_{L_w} + C_{L_c} + C_J$$

3. General Camber Distribution

We assume a general camber shape to be made up of a series of flap-like elements. Then we take J elements and evaluate the lift coefficient for each, where $C_{L_{\delta_p}}$ represents the lift for a flap located at $x_f = x_p$.

We now define the slope of each element as y'_{co}, y'_{c1} . . . . and obtain for the lift coefficient due to camber

$$C_{L_c} = -y'_{co}\, C_{L_a} + (y'_{co} - y'_{c1})\, C_{L_{\delta_1}} + \cdots$$

$$= -y'_{co}\, C_{L_a} + \sum_{1}^{J-1} (y'_{c(i-o)} - y'_{ci})\, C_{L_{\delta_1}}$$

B. THICKNESS

1. Basic Solution

The thickness case is considered in the same spirit as the camber, by approximating the airfoil by a trapezoidal shape. For the basic thickness case we have boundary conditions similar to camber except that the left-hand v distribution is of opposite sign and the jet angle at the trailing edge zero.

Thus the addition $u^+ - u^-$ term becomes

$$N_i^* = M(\bar{\xi}_i^+) - M^-(\bar{\xi}_i^+) - M(\bar{\xi}_i^-) + M^-(\bar{\xi}_i^-) \qquad i = 1 \ldots N$$

while $V_o = 0$ so that the linear set is

$$\sum_{i=1}^{N} (E_{in} + F_{in})\, V_i = -N_i^* \qquad n = 1 \ldots N$$

2. Lift Coefficient

This follows exactly the same development as the camber case with the thickness term C_{L_t} given by

$$\frac{\pi}{2} \frac{c}{h} (a+k)\, C_{L_t} = \int_{-1}^{\xi_t^-} K(a,t)dt - \int_{\xi_t^+}^{1} K(a,t)dt$$

integrated to give

$$\frac{\pi}{2} \frac{c}{h} (a+k)\, C_{L_t} = I(\xi_t^-, -1) - I(1, \xi_t^+)$$

3. General Thickness Distribution

We assume the distribution to consist of a number of flat-sided

elements and obtain a summation for the total thickness lift slope exactly analogous to that for the camber, using the appropriate values of $C_{L_{t_i}}$.

C. GENERAL OBSERVATIONS ON THICKNESS AND CAMBER

The effects of thickness and camber on a jet-flapped airfoil are of great significance technologically. In the first place, the consequences of a finite thickness in a real airfoil must be considered, especially as in ground effect the thickness contributes to lift. Next we note that the camber distribution is an important means of controlling the airfoil pitching moments, which are large for jet flap airfoils and present serious stabilizing problems for actual design arrangements.

Finally, the ability to vary the pressure distribution on the airfoil by means of these two effects provides one with a means of reducing or eliminating some of the adverse effects caused by boundary layer separation due to unfavorable pressure gradients. In particular, the strong adverse gradients on the upper surface near the leading edge due to the nose flow frequently cause a nose separation, which is most readily controlled by large local leading edge camber (nose droop), which can move the stagnation point to the leading edge -- in this analysis this would correspond to eliminating the nose source. Additional control may be achieved by variation of the airfoil nose radius.

Of course, this analysis cannot directly handle the non-linear problem associated with a finite nose radius; in addition the airfoil pressure distribution evaluated here will have logarithmic peaks at each discontinuity in slope. However, it is relatively easy to develop local perturbation solutions for the flow around a finite nose radius and to 'smooth' the airfoil pressure distribution by similar methods:

this would be essential for any boundary layer calculations. Evidently, these are developmental techniques so are not discussed here.

The numerical solution of the thickness and camber cases was not carried out, principally because of the relatively long computer time required. The solution for any particular point would not require more time than a point for the basic case, but for sufficient generality one would require solutions for 'kinks' on at least 10 stations on the airfoil for both thickness and camber which would have increased the computer time by a factor of 15 to 20. In any case the actual numerical solutions are not essential to this paper which is concerned with the development of the general theory.

We note that asymptotic solutions, valid for $C_J < \cdot 5$, can be derived from the standard ground effect solutions for simple airfoils with thickness (Tani, Ref. 14). These are developed on identical lines to those for the flat plate airfoil using the results for $C_{L_\alpha}(h/c, t/c)$. Similarly one may derive results for $C_J \to 0$ from the ground effect solution for the simple flapped airfoil, which will be directly related to our camber solutions.

VIII. SUGGESTIONS FOR FURTHER WORK

A. Linear Inviscid Theory

The present paper, being an exact solution, effectively exhausts any further analytical work within this framework. From the engineering aspect it would be useful to compute some standard cases for thickness and camber. It would also be worthwhile, using the computed values of $C_{L_w}(C_J, G)$, to derive an approximate closed functional form for C_{L_w} in terms of its parameters. This would be valuable for optimization studies.

We have already shown how the solutions for small C_J can be obtained by perturbing about the known solutions for $C_J = 0$. It would be instructive to construct a similar perturbation about the known Spence solutions ($G = 1$) for the case of G near 1. The fact that $h/c = 3$ corresponds to $G = .95$ suggests that such a perturbation might be valid down to relatively low h/c. This might be conducted on the following lines:

Assume $v(\xi) = v^{(o)}(\xi) + (1-G)v^{(1)}(\xi) + 0((1-G)^2)$, where $v^{(o)}(\xi)$ is the solution for $G = 1$ and $v^{(1)}(\xi)$ is a function $O(1)$. We note that at $\xi = 1$, the flap-type singularity dominates, and we can immediately write $v^{(1)}(1) = 0$ and also obtain an asymptotic result for $\frac{dv^{(1)}}{d\xi}$ near 0.

Now we note

$$\frac{\pi^2 G^2}{4} C_{L_w} = (a+k)\int_{-\infty}^{\infty} K(a,t)v(t)dt$$

with

$$\frac{\pi^2}{4} C_{L_w}^{(o)} = \int_{-\infty}^{\infty} \lim_{a \to o} \{(a+k)K(a,t)\} v^{(o)}(t)dt$$

Thus we have

$$\frac{\pi^2}{4} C_{L_w} = \int_{-\infty}^{\infty} (a+k)K(a,t) \{v^{(o)}(t) + (1-G) v^{(1)}(t) + \ldots \} dt$$

$$\sim \int_{-\infty}^{\infty} (a+k)K(a,t)v^{(o)}(t)dt + (1-G) \int_{-\infty}^{\infty} (a+k)K(a,t)v^{(1)}(t)dt$$

Now $K(a,t)$ has logarithmic singularities at $t^2 = 1$ and then decays quite rapidly. Thus we might expect that, of the two integrals, the former, having $v^{(o)}(1) = 1$ will be much more significant than the latter with $v^{(1)}(1) = 0$.

In this case we might approximate C_{L_w} by

$$\frac{\pi^2}{4} C_{L_w} \approx \int_{-\infty}^{\infty} (a+k)K(a,t) v^{(o)}(t) dt$$

which is a direct quadrature, using the Spence result for $v^{(o)}(t)$.

The significance of investigating approximations of this type, when the exact solution is known, is that a direct check on accuracy of the approximation is obtained, which is very valuable if the same technique is applied to a more complex situation where the exact solution cannot be determined.

B. NON-LINEAR INVISCID THEORY

The non-linear case has not been solved, with or without ground plane. It is important to obtain either an exact or second order theory, particularly for the jet immediately behind the trailing edge. The non-linearities in the jet position and its curvature, and in the dynamic boundary condition are essential to the problem, but the airfoil may still be taken as of zero thickness. The present solution could probably be used as a basic solution to initiate some perturbation scheme.

C. VISCOUS EFFECTS

It is of great interest to study the entrainment effects if the jet wake is considered to be turbulent. A first order approach to this would be to consider the linear potential solution developed in this paper with some additional sink distribution in the wake. If this distribution were known a priori, it could readily be added to the computer program as the start of an iterative process. Whether this is convergent is not known, although the above procedure has been shown to be successful in the case of jet flow along rigid walls.

REFERENCES

1. Davidson, I. M.: The Jet Flap. J. Roy. Aero. Soc., Vol. 60, No. 1, 1956.

2. Spence, D. A.: The Lift Coefficient of a Thin Jet-Flapped Wing. Proc. Roy. Soc. Series A, Vol. 238, No. 121, 1956.

3. Stratford, B. S.: Early Thoughts on the Jet Flap. Aero. Quart. Vol. VII, Part 1, 1956.

4. Foley, W. M.: An Experimental Study of Jet-Flap Thrust Recovery. Stanford University, Dept. of Aero. and Astro., 1962.

5. Pivko, Svetopolk: Effect of a Jet Issuing from the Trailing Edge on the Aerodynamic Properties of a Thin Airfoil. Tehnika (Masinstvo) Vol. 9, No. 9, Belgrad, 1960. Astia Translation AD 286 194.

6. Erickson, J. C.: A Theory for Unsteady Motions of Jet Flapped Thin Airfoils. Cornell University, Grad. School of Aerospace Eng. Rep., 1962.

7. Das, A.: Tragflachen Theorie Fur Tragflugel Mit Strahlklappen. Jahrbuch 1960 W.G.L.

8. Huggett, D. J.: The Ground Effect on the Jet Flap in Two Dimensions. Aero. Quart. Vol. X, 1959.

9. Williams, P. G.: A Note on the Lift of a Jet-Flap Aerofoil near the Ground. A.R.C. 23,821, 1962.

10. Lissaman, P.B.S.: Aerodynamic Characteristics of Jet-Flapped Airfoils in Ground Effects. Vehicle Research Corporation Report No. 18, 1964.

11. Muskhelishvili, N. I.: Singular Integral Equations, Second Ed. Moscow, 1946. Aero. Research Lab., Australia, Translation No. 12.

12. Spence, D. A.: Some Simple Results for Two-Dimensional Jet-Flap Aerofoils. Aero. Quart. Vol.

13. Tricomi, F. G.: Integral Equations, Interscience Publishers Inc., First Ed. New York, 1957.

14. Tani, I.; Taima, M.; Simidu, S.: The Effect of the Ground on the Aerodynamic Characteristics of a Monoplane Wing. Aero. Research Inst. Tokyo, No. 156, 1937.

APPENDIX

EVALUATION OF THE KERNEL INTEGRAL

We consider

$$I(B,A) = \int_A^B \left(\frac{a-t}{k+t} \log \frac{t-1}{t+1} - \frac{2}{k+t} \right) dt \qquad k > 1, \quad B > A$$

We note that the integrand is logarithmically singular at ± 1. At $t = -k$ however, because of the relationship $(a+k)\log \frac{k+1}{k-1} = 2$, the integrand equals $\log \frac{k+1}{k-1}$. We consider three different ranges of integration; and as a preliminary standard form introduce the integral:

$$\int_a^b \frac{1}{t} \log (1-t)\, dt = B_1(b) - B_1(a) \qquad a, b \leq 1$$

where $B_1(t) = -\sum_1^\infty \frac{t^n}{n^2} \qquad |t| \leq 1$

since $\frac{dB_1}{dt}(t) = -\frac{1}{t} \sum_1^\infty \frac{t^n}{n} = \frac{1}{t} \log (1-t)$

and $B_1(0) = 0$, while $B_1(1) = \pi^2/6 = \pi^2 B_1$ where B_1 is the first Bernoulli Number.

Case 1: $A, B \geq 1$

$$I(B,A) = \int_A^B \left\{ (a+k) \frac{1}{k+t} \log \left(\frac{t-1}{t+1}\right) - \log \left(\frac{t-1}{t+1}\right) - \frac{2}{k+t} \right\} dt$$

For the first term we write, by changing the variable,

$$I_1 = \int_{A+k}^{B+k} \left\{ \frac{1}{x} \log\left(1 - \frac{k+1}{x}\right) - \frac{1}{x} \log\left(1 - \frac{k-1}{x}\right) \right\} dx$$

$$= \int_{\frac{A+k}{k+1}}^{\frac{B+k}{k+1}} \frac{1}{x} \log\left(1 - \frac{1}{x}\right) dx - \int_{\frac{A+k}{k-1}}^{\frac{B+k}{k-1}} \frac{1}{x} \log\left(1 - \frac{1}{x}\right) dx$$

Then by inverting the argument of the integrand and applying the standard integral we get:

$$I_1 = B_1\left(\frac{k+1}{k+A}\right) - B_1\left(\frac{k+1}{k+B}\right) - B_1\left(\frac{k-1}{k+A}\right) + B_1\left(\frac{k-1}{B+k}\right)$$

The remaining two terms of the integral are integrated by elementary methods to give

$$I(B,A) = \left\{ B_1\left(\frac{k+1}{k+A}\right) - B_1\left(\frac{k+1}{k+B}\right) - B_1\left(\frac{k-1}{k+A}\right) + B_1\left(\frac{k-1}{B+k}\right) \right\} (a+k)$$

$$- B \log\left(\frac{B-1}{B+1}\right) + \log\left(B^2-1\right) + A \log\left(\frac{A-1}{A+1}\right) - \log\left(A^2-1\right)$$

$$- 2 \log\left(\frac{B+k}{A+k}\right)$$

Then, taking the various limits, we get

$$I(\infty,1) = (a+k)\left\{ B_1(1) - B_1\left(\frac{k-1}{k+1}\right) \right\} + 2 + 2 \log(k+1) - 2 \log 2$$

Case 2: $-1 < A, B \leq 1$

Defining I_1 similarly, except with the moduli of the logarithmic arguments we write

$$I_1 = \int_{\frac{A+k}{k+1}}^{\frac{B+k}{k+1}} \frac{1}{x} \log \left|1 - \frac{1}{x}\right| dx - \int_{\frac{A+k}{k-1}}^{\frac{B+k}{k-1}} \frac{1}{x} \log \left|1 - \frac{1}{x}\right| dx$$

$$= \int_{\frac{A+k}{k+1}}^{\frac{B+k}{k+1}} \frac{1}{x} \log |1-x| dx - \int_{\frac{A+k}{k+1}}^{\frac{B+k}{k+1}} \frac{1}{x} \log |x| dx - \int_{\frac{A+k}{k-1}}^{\frac{B+k}{k-1}} \frac{1}{x} \log \left|1 - \frac{1}{x}\right| dx$$

Now, defining $\int_a^b \frac{1}{x} \log x \, dx = \mathrm{Li}(b) - \mathrm{Li}(a)$ $\qquad a, b > 0$

and using the standard integral, we get

$$I(B,A) = \left\{B_1\left(\frac{k+B}{k+1}\right) - B_1\left(\frac{k+A}{k+1}\right) - \mathrm{Li}\left(\frac{k+B}{k+L}\right) + \mathrm{Li}\left(\frac{k+A}{k+1}\right)\right.$$

$$\left. - B_1\left(\frac{k-1}{k+A}\right) + B_1\left(\frac{k-1}{k+B}\right)\right\}(a+k) - B \log \left|\frac{B-1}{B+1}\right| + \log (B^2-1)$$

$$+ A \log \left|\frac{A-1}{A+1}\right| - \log (A^2-1) - 2 \log \left|\frac{B+k}{A+k}\right|$$

Then, taking the various limits, we get

$$I(1, \xi_f^+) = (a+k) \left\{B_1(1) - B_1\left(\frac{k+\xi_f^+}{k+1}\right) - \mathrm{Li}(1) + \mathrm{Li}\left(\frac{k+\xi_f^+}{k+1}\right)\right.$$

$$\left. - B_1\left(\frac{k-1}{k+\xi_f^+}\right) + B_1\left(\frac{k-1}{k+1}\right)\right\} + 2 \log 2 + \xi_f^+ \log \frac{\xi_f^+ - 1}{\xi_f^+ + 1}$$

$$- \log (\xi_f^{+2}-1) - 2 \log \left|\frac{k+1}{\xi_f^+ + 1}\right|$$

Case 3: $-1 < A, B < 1$

Using an analysis similar to Case 2 we get

$$I(\bar{\xi}_f, -1) = (a+k)\left\{B_1\left(\frac{\bar{\xi}_f+k}{1+k}\right) - B_1\left(\frac{k-1}{k+1}\right) + \mathrm{Li}\left(\frac{k-1}{k+1}\right) - \mathrm{Li}\left(\frac{k+\bar{\xi}_f}{k+1}\right)\right.$$

$$\left. - B_1(1) + B_1\left(\frac{k-1}{k+\bar{\xi}_f}\right)\right\} - \bar{\xi}_f \log\left|\frac{\bar{\xi}_f - 1}{\bar{\xi}_f + 1}\right| + \log\left(\bar{\xi}_f^{-2} - 1\right)$$

$$- 2\log 2 - 2\log\left|\frac{1+k}{\bar{\xi}_f + k}\right|$$

Case 4: $-k \leq A, B \leq -1$

We write I_1 as

$$I_1 = \int_{A+k}^{B+k} \left(\frac{1}{x}\log\left(1 - \frac{1}{k+1}\right) - \frac{1}{x}\log\left(1 - \frac{x}{k-1}\right) + \frac{1}{x}\log\frac{k+1}{k-1}\right) dx$$

$$= \int_{\frac{A+k}{k+1}}^{\frac{B+k}{k+1}} \frac{1}{x}\log(1-x)\,dx - \int_{\frac{A+k}{k-1}}^{\frac{B+k}{k-1}} \frac{1}{x}\log(1-x)\,dx + \int_A^B \frac{2}{(k+x)}\,\frac{dx}{(a+k)}$$

Observing first that the last expression cancels the third term of $I(B,A)$ we get

$$I(B,A) = \left\{B_1\left(\frac{k+B}{k+1}\right) - B_1\left(\frac{k+A}{k+1}\right) - B_1\left(\frac{k+B}{k-1}\right) + B_1\left(\frac{k+A}{k-1}\right)\right\}$$

$$- B\log\left|\frac{B-1}{B+1}\right| - \log\left(B^2 - 1\right) + A\log\left|\frac{A-1}{A+1}\right| - \log\left(A^2 - 1\right)$$

Then, taking the various limits, we get

$$I(-1,-k) = (a+k)\left\{B_1\left(\frac{k-1}{k+1}\right) - B_1(1)\right\} + 2\log 2$$

$$+ (k-1)\log(k-1) - (k+1)\log(k+1)$$

LIST OF FIGURES

JET FLAP GEOMETRY

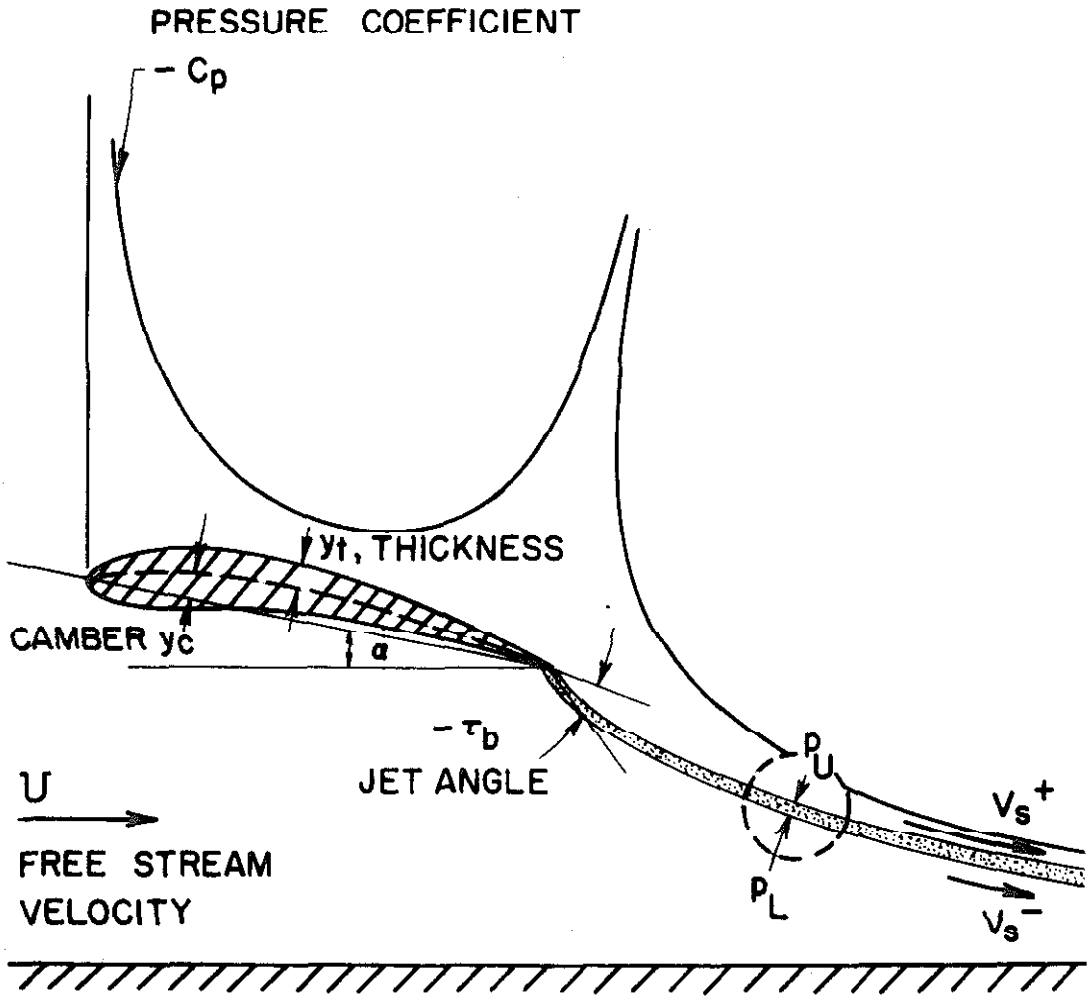

FIG. 1

LINEARIZED SKETCH IN REAL PLANE SHOWING BOUNDARY CONDITIONS

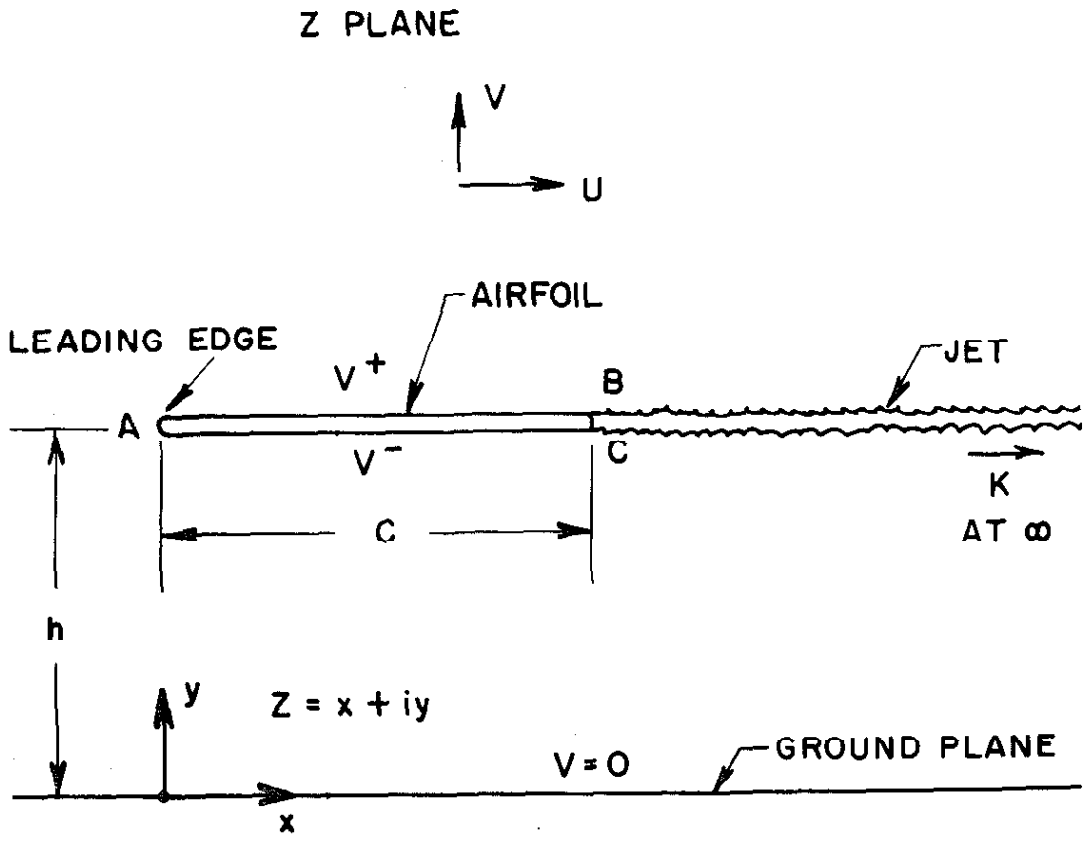

FIG. 2

$Z \Longleftrightarrow \zeta$ MAPPING

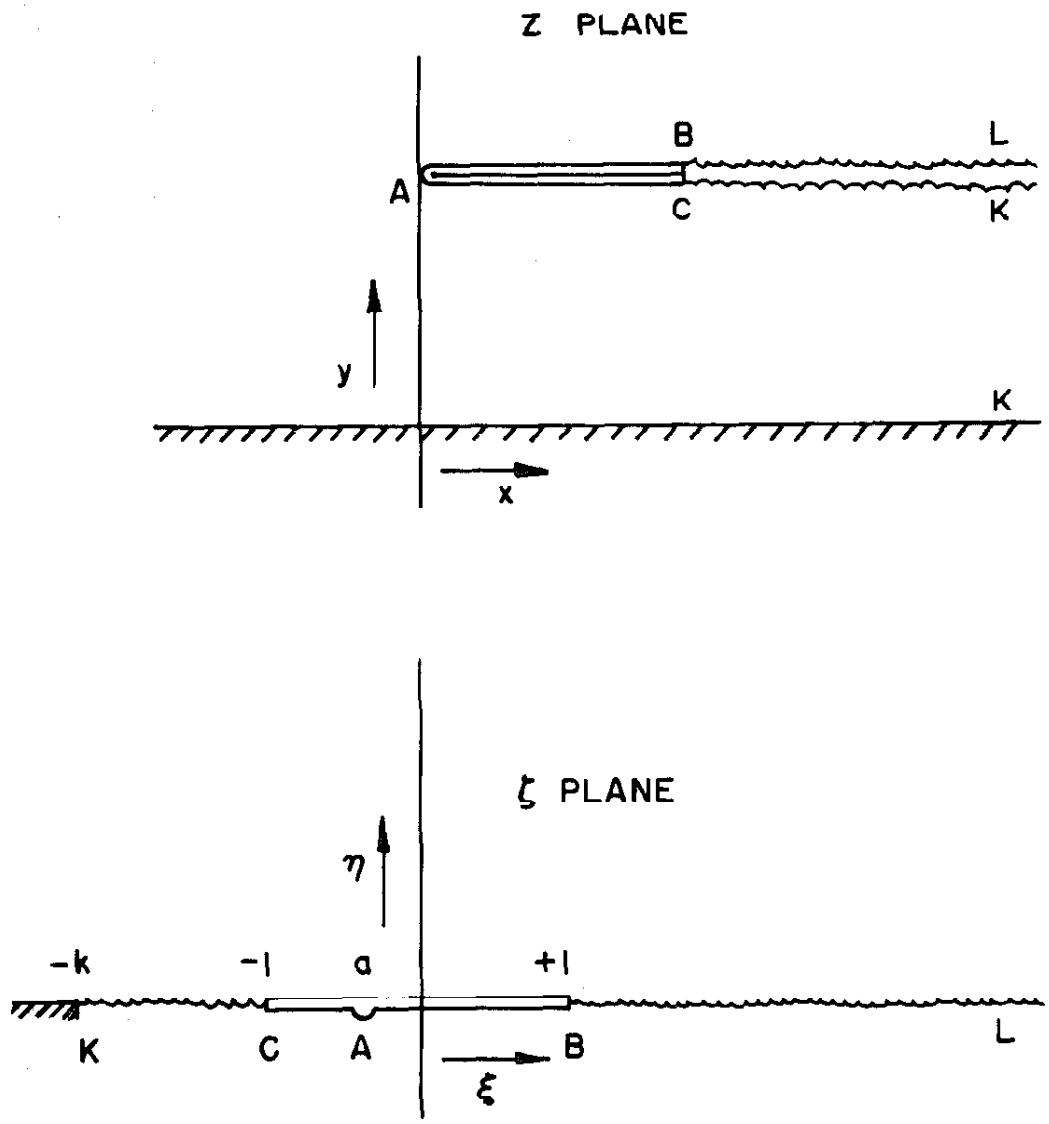

FIG. 3

SCALING OF TRANSFORMATION

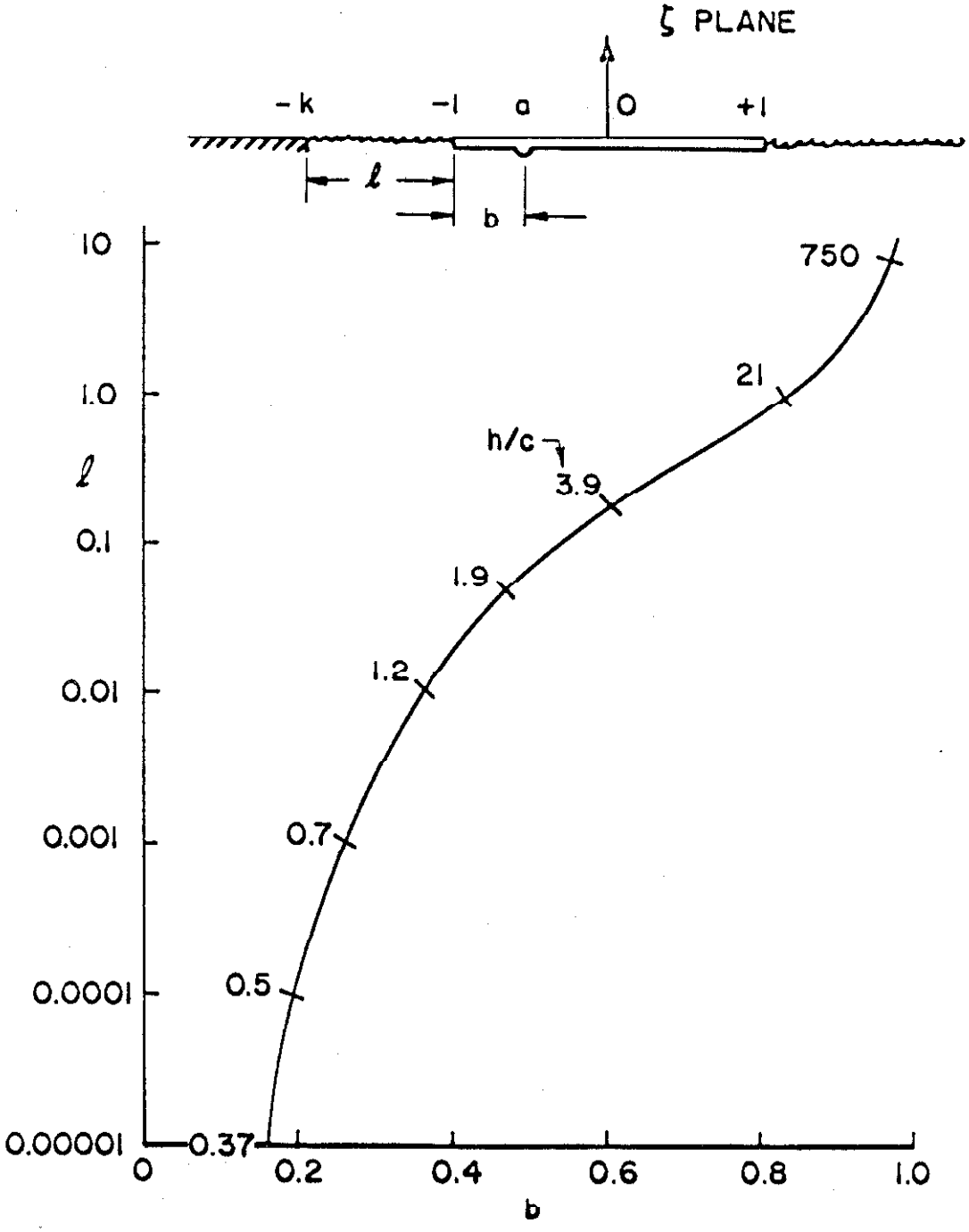

FIG. 4

BASIC JET ANGLE BOUNDARY CONDITIONS

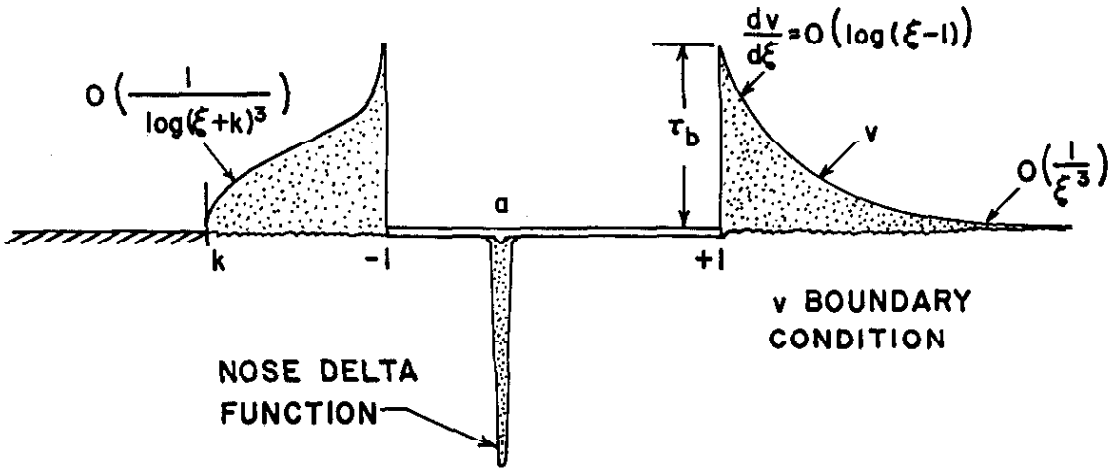

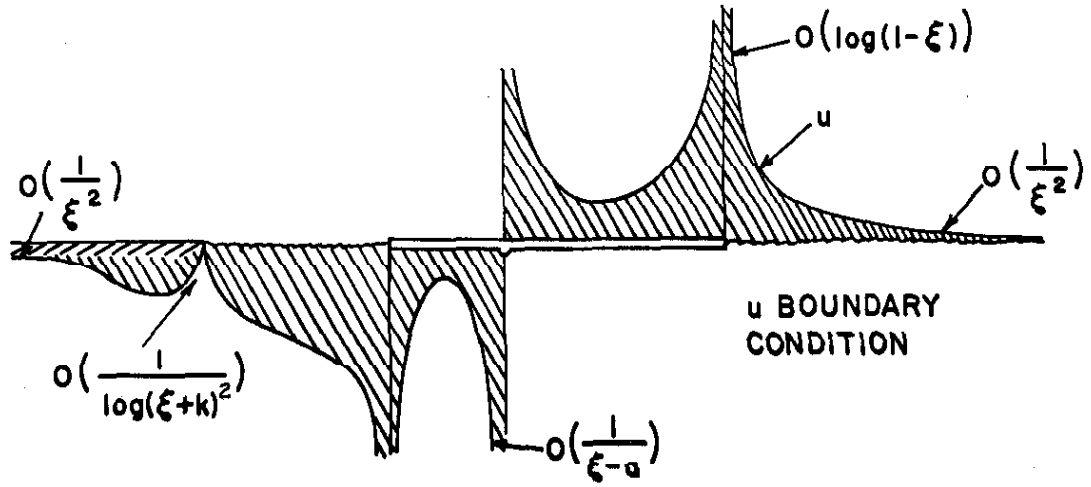

FIG. 5

FORCE SYSTEM ON AIRFOIL

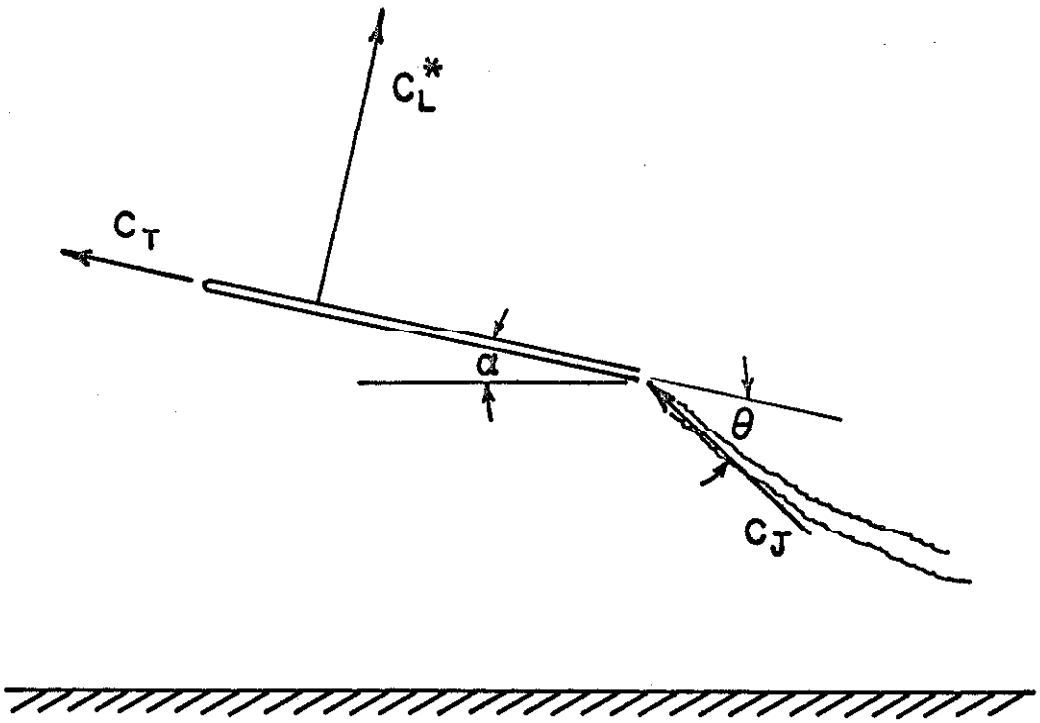

FIG. 6

APPROXIMATE V FUNCTION

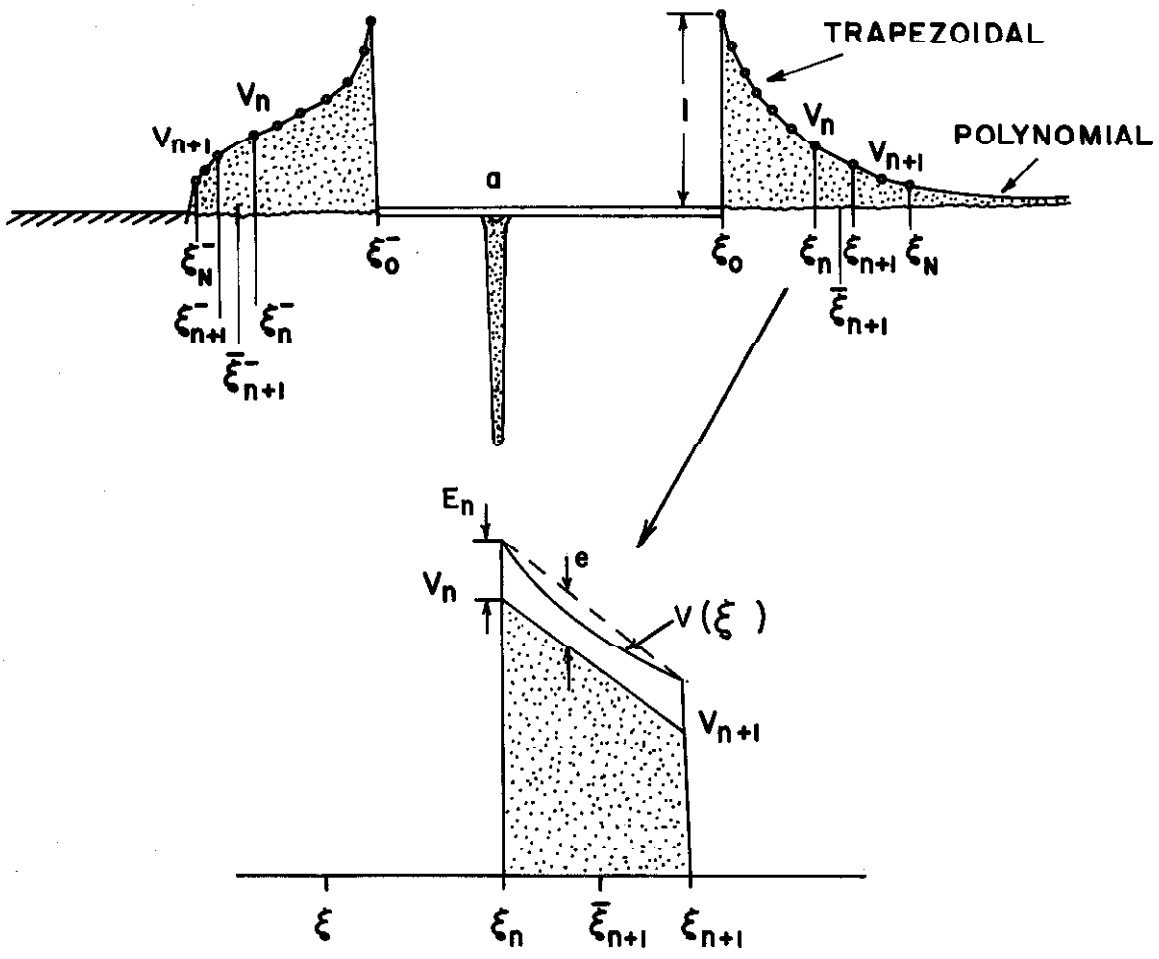

ELEMENTARY TRAPEZOIDAL
DRISTRIBUTION

FIG. 7

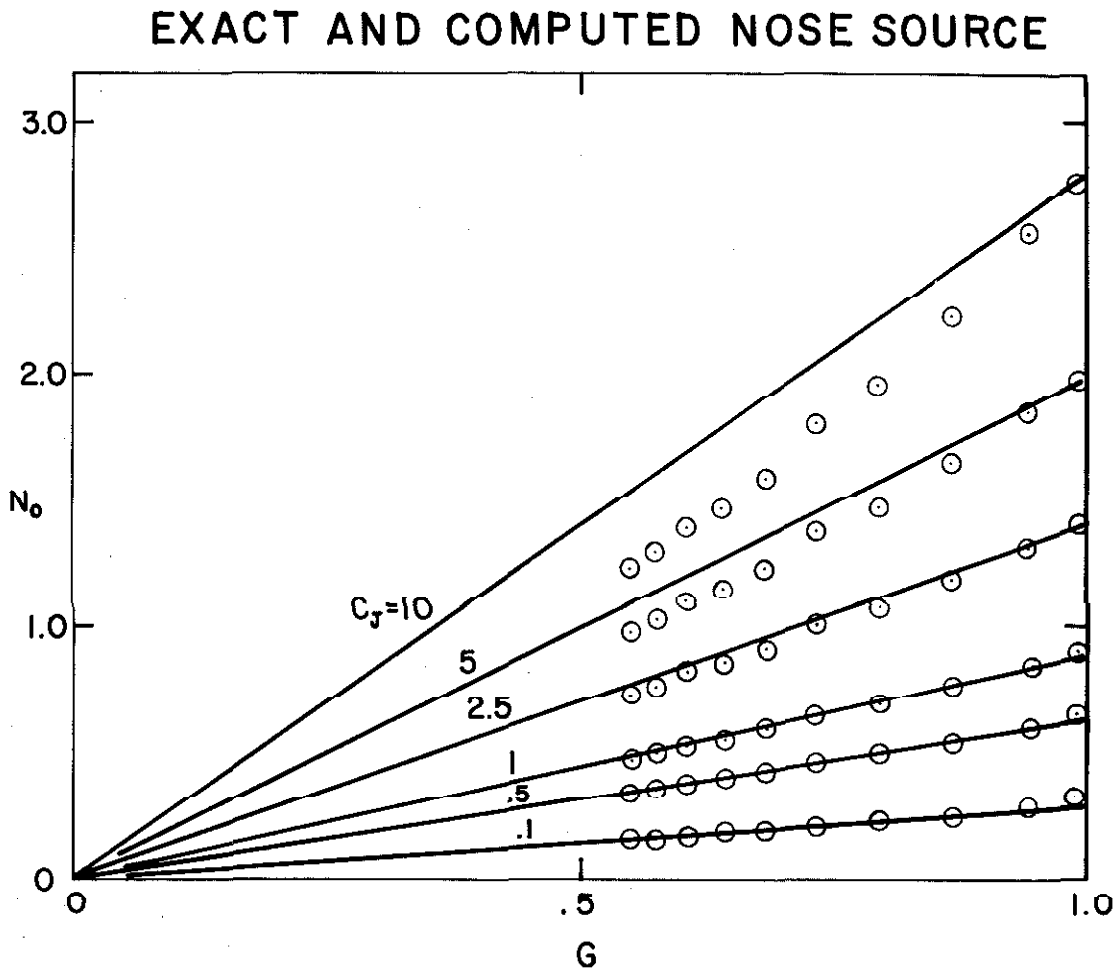
EXACT AND COMPUTED NOSE SOURCE
3.0
2.0
1.0
0
N_o
C_J=10
5
2.5
1
.5
.1
0
.5
1.0
G

FIG. 8

GENERATED V CURVES (R.H.S.)

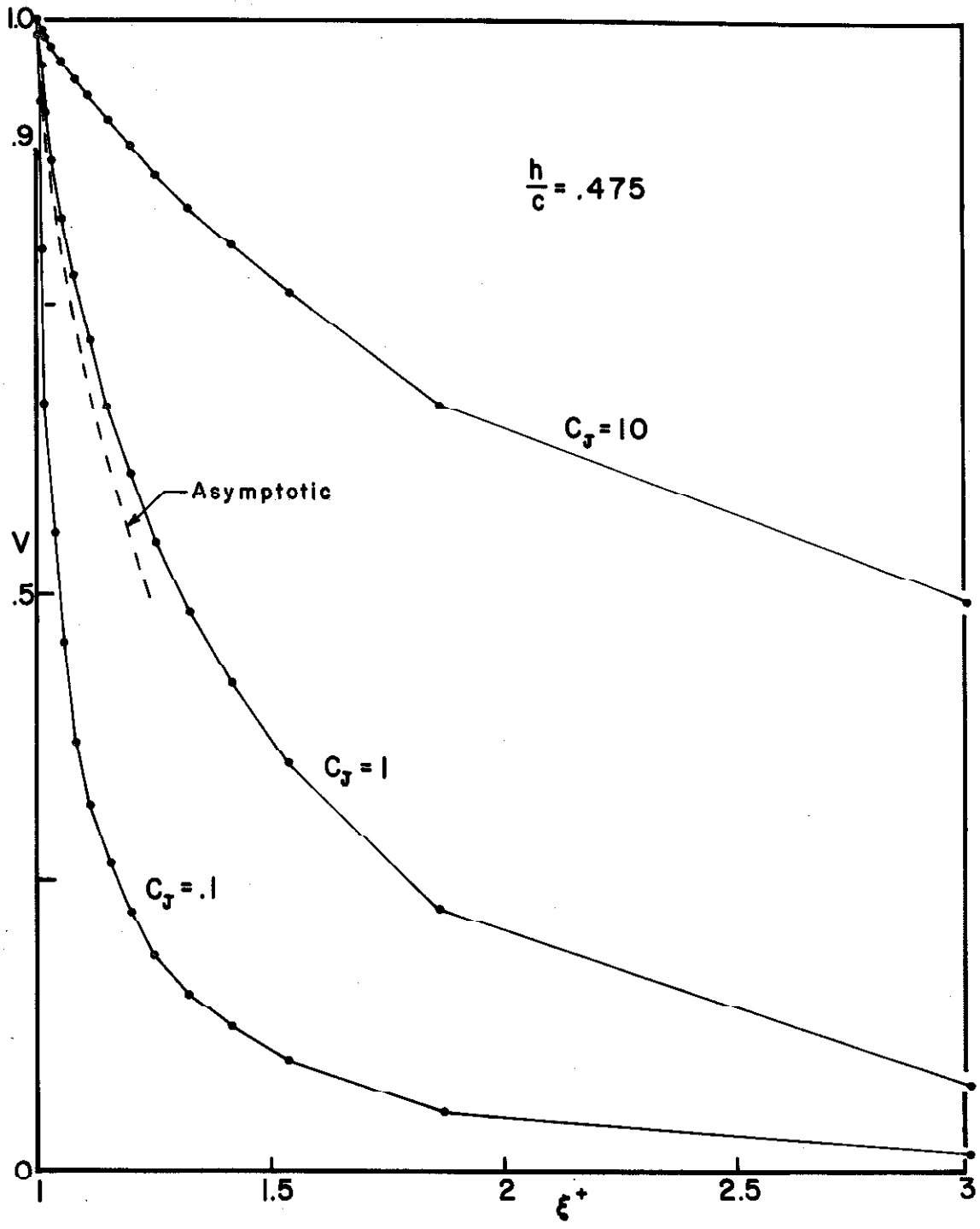

FIG. 9

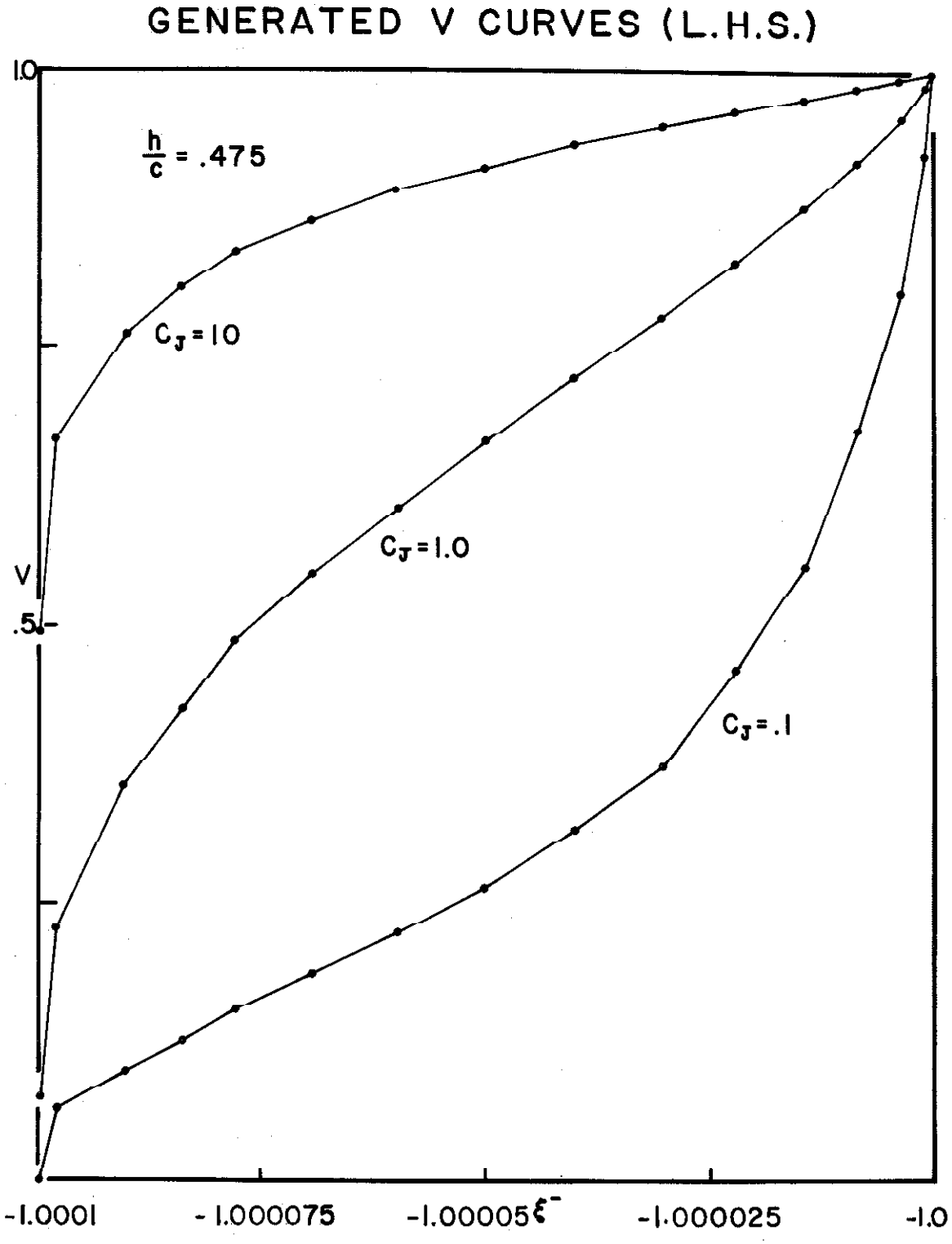
GENERATED V CURVES (L.H.S.)
1.0
h/c = .475
C_J = 10
C_J = 1.0
C_J = .1
V
.5
-1.0001
-1.000075
-1.00005
-1.000025
-1.0
ε⁻

FIG. 10

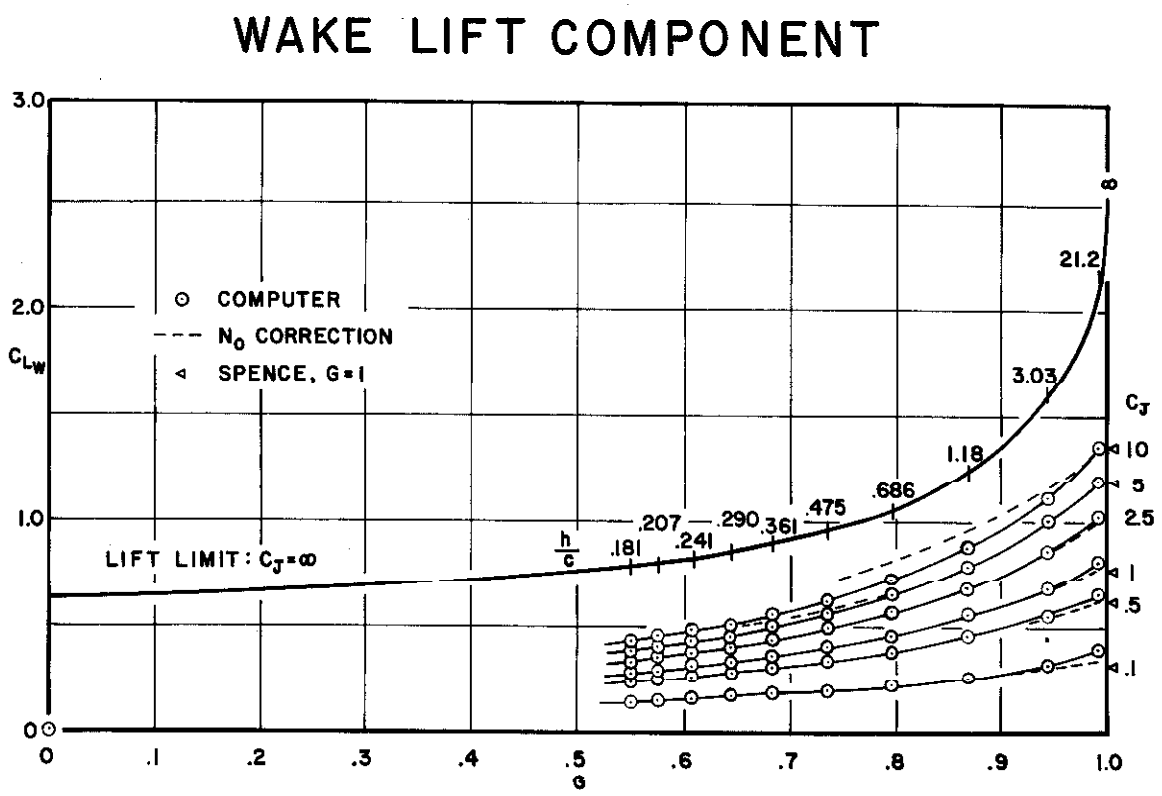
WAKE LIFT COMPONENT
3.0
2.0
1.0
0
C_{L_W}
COMPUTER
N_0 CORRECTION
SPENCE, G=1
LIFT LIMIT: $C_J=\infty$
$\frac{h}{c}$
.181
.207
.241
.290
.361
.475
.686
1.18
3.03
21.2
∞
C_J
10
5
2.5
1
.5
.1
0
.1
.2
.3
.4
.5
.6
.7
.8
.9
1.0
G

FIG. 11

LIFT CURVES IN GROUND EFFECT

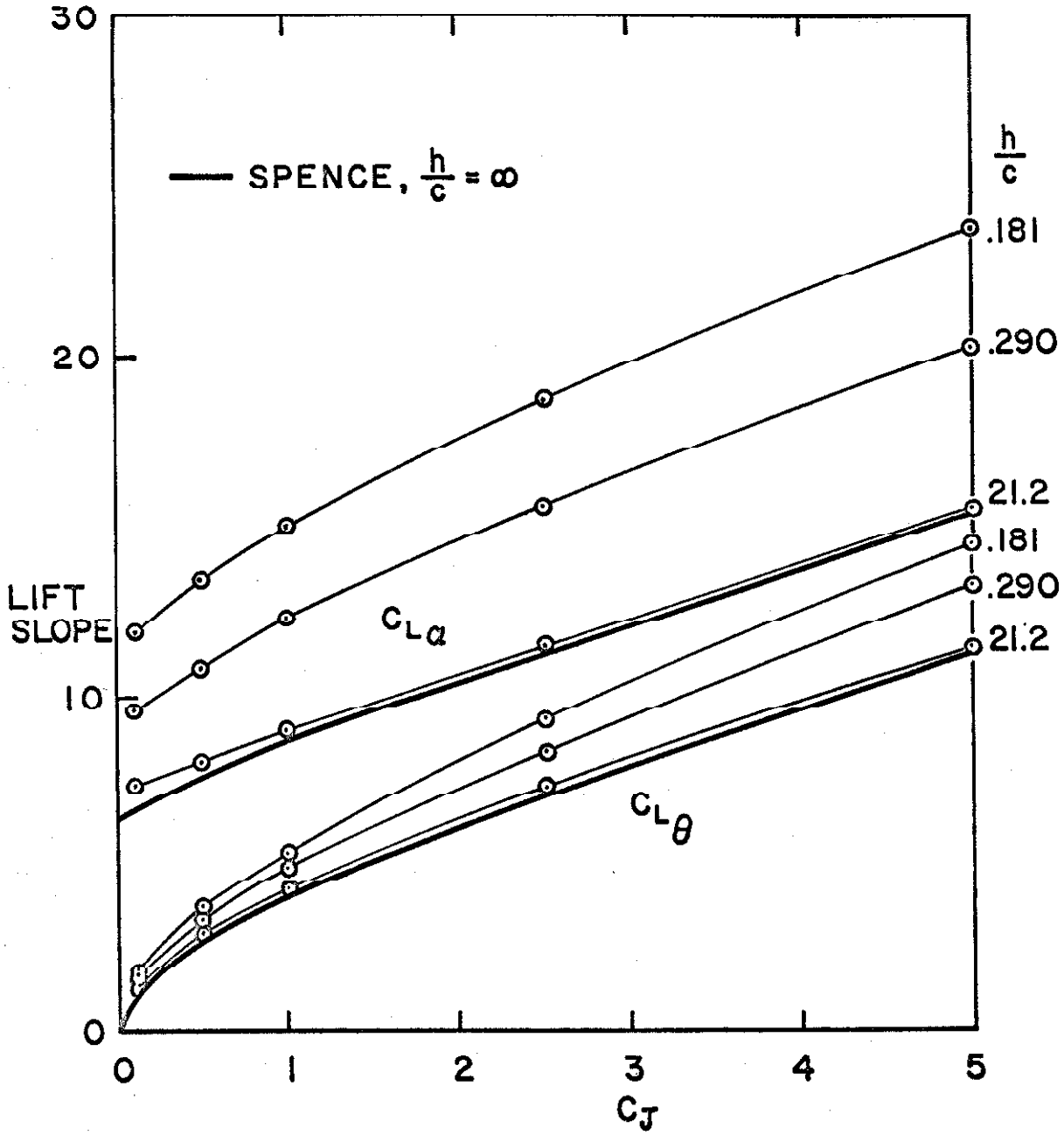

FIG. 12

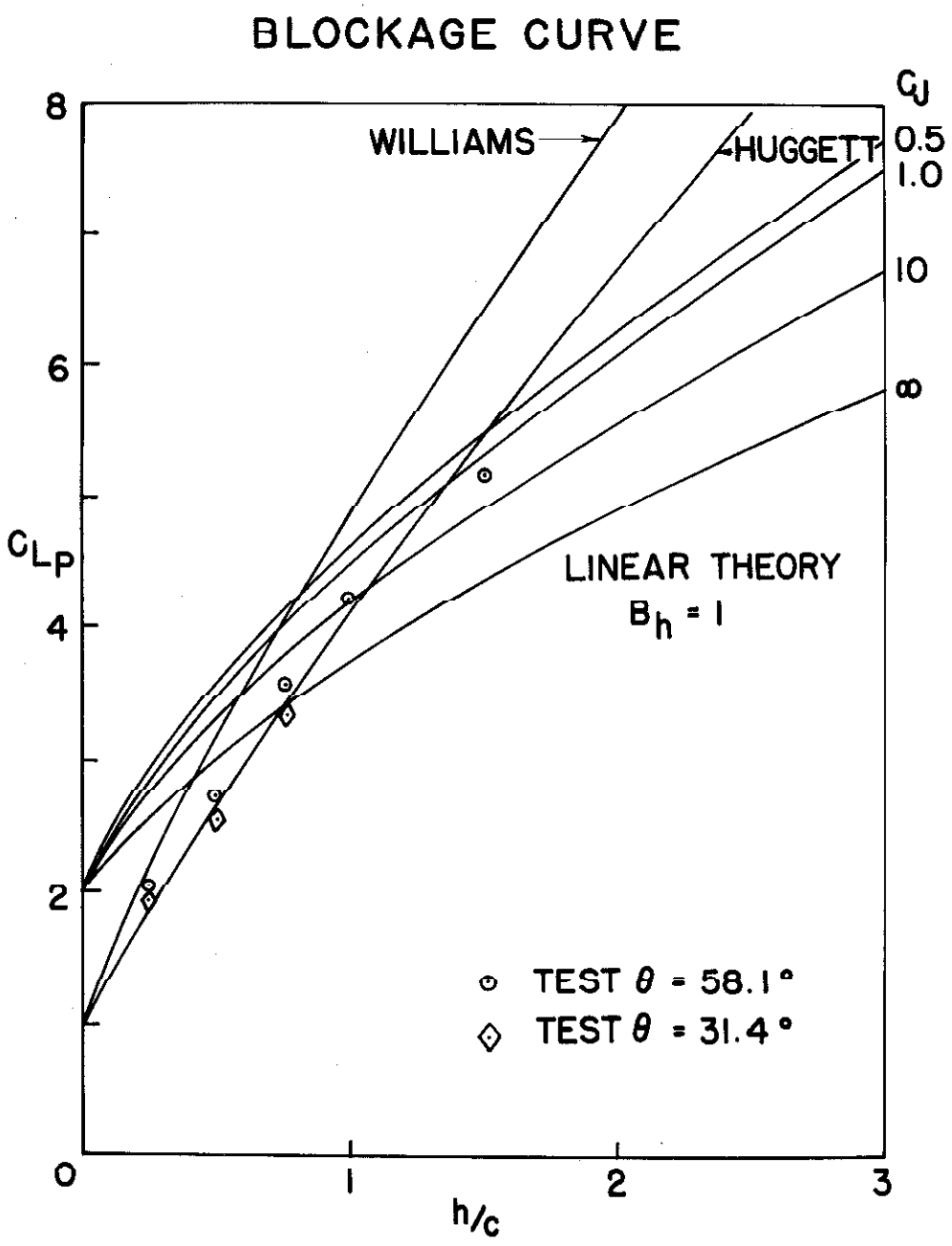
BLOCKAGE CURVE
C_J
0.5
1.0
10
∞
WILLIAMS
HUGGETT
LINEAR THEORY
$B_h = 1$
C_{L_P}
8
6
4
2
0
1
2
3
h/c
TEST θ = 58.1°
TEST θ = 31.4°

FIG. 13

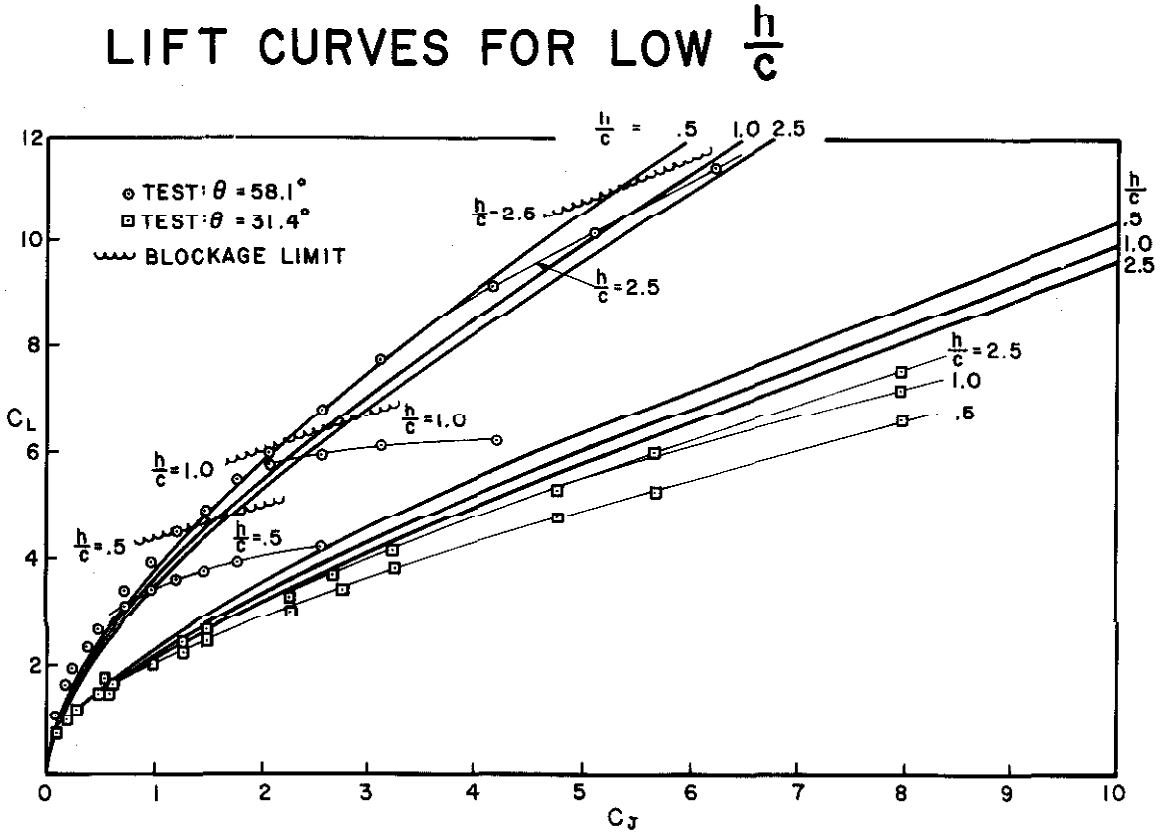
LIFT CURVES FOR LOW h/c
h/c = .5 1.0 2.5
⊙ TEST: θ = 58.1°
⊡ TEST: θ = 31.4°
BLOCKAGE LIMIT
h/c=2.6
h/c=2.5
h/c=1.0
h/c=.5
h/c=1.0
h/c=.5
h/c=2.5
1.0
.5
h/c
.5
1.0
2.5
C_L
C_J
0
1
2
3
4
5
6
7
8
9
10
2
4
6
8
10
12

FIG. 14

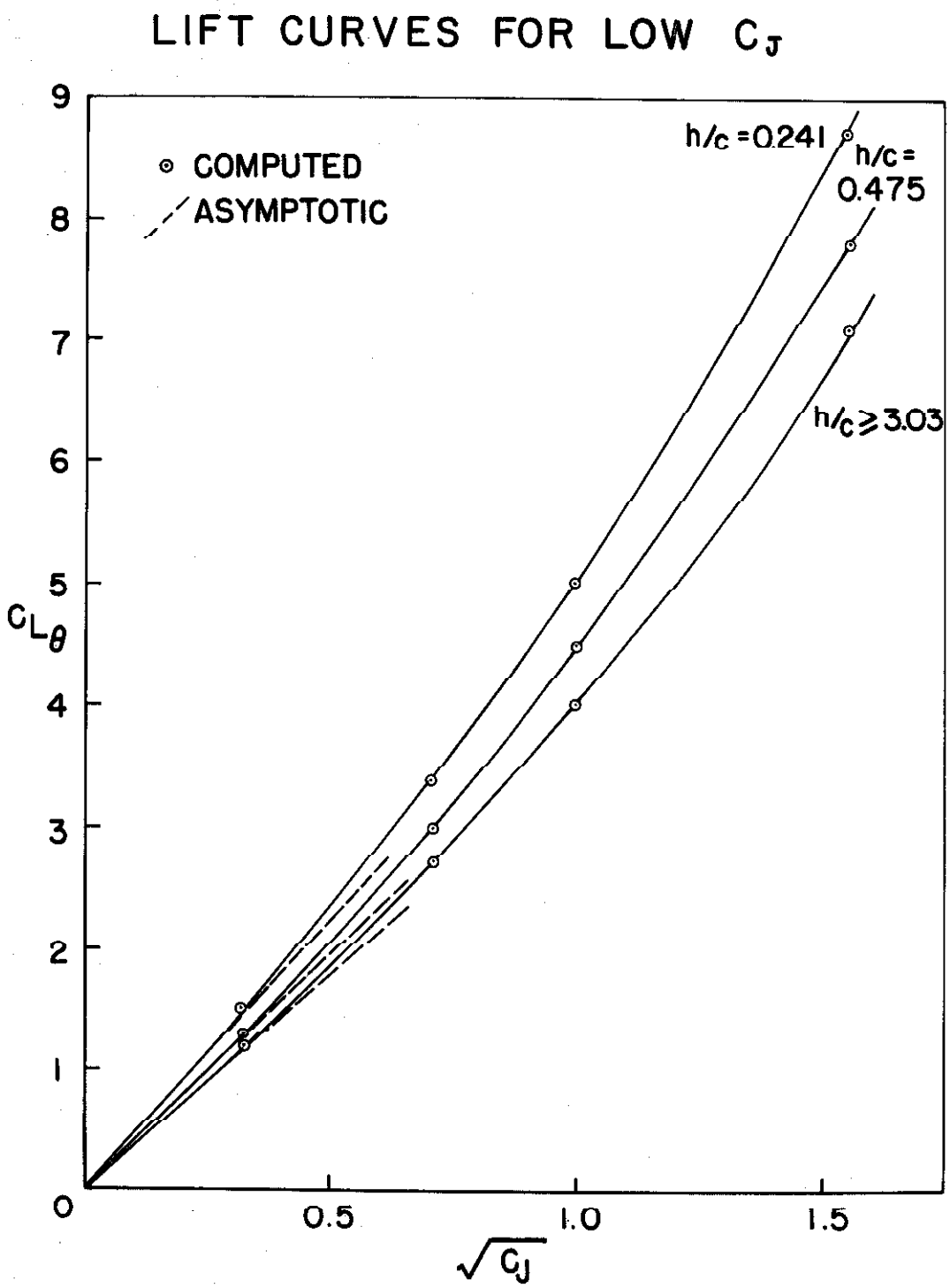
LIFT CURVES FOR LOW C_J
COMPUTED
ASYMPTOTIC
h/c =0.241
h/c = 0.475
h/c ≥ 3.03
C_{L_θ}
$\sqrt{C_J}$
0
1
2
3
4
5
6
7
8
9
0.5
1.0
1.5

FIG. 15

BASIC CAMBER BOUNDARY CONDITIONS

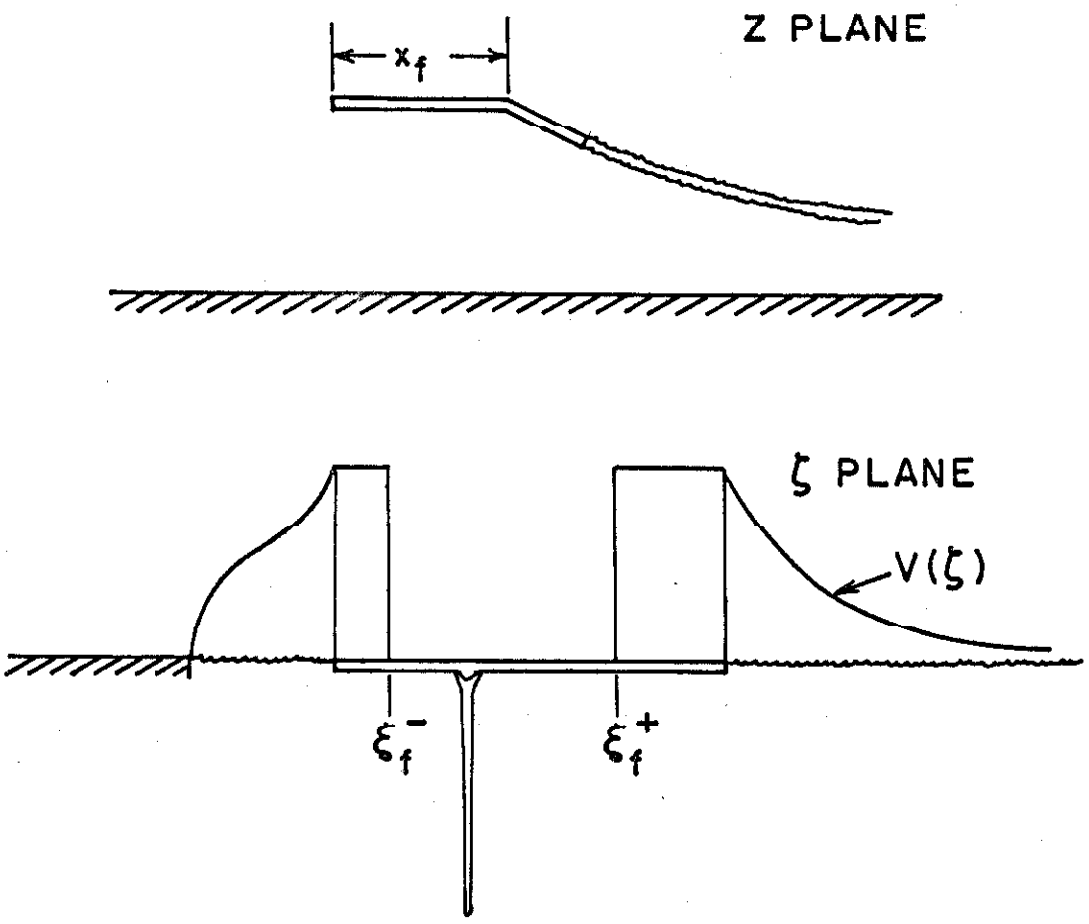

FIG. 16